A mathematical model of the pulsed coil system of a tokamak reactor

J. Raeder

IPP 4/174 January 1979

MAX-PLANCK-INSTITUT FÜR PLASMAPHYSIK

8046 GARCHING BEI MÜNCHEN

MAX-PLANCK-INSTITUT FÜR PLASMAPHYSIK

GARCHING BEI MÜNCHEN

A mathematical model of the
pulsed coil system of a tokamak reactor

J. Raeder

IPP 4/174 January 1979

Die nachstehende Arbeit wurde im Rahmen des Vertrages zwischen dem Max-Planck-Institut für Plasmaphysik und der Europäischen Atomgemeinschaft über die Zusammenarbeit auf dem Gebiete der Plasmaphysik durchgeführt.

IPP 4/174

A mathematical model of the pulsed coil system of a tokamak reactor.

J. Raeder

January 1979

Abstract

A mathematical model of the pulsed magnetic circuits of a tokamak is set up for use as part of the SISYFUS comprehensive computer code of IPP, which models a complete tokamak fusion power plant and is to be used for parametric systems and design studies.

The first section gives a brief review of the features characteristic of pulsed tokamak coil systems and their mathematical description by flux functions, magnetic field distributions and stored magnetic energies.

In the second section a tokamak is treated simply as a system of resistive coils which are inductively coupled. The definition of inductances and the derivation of circuit equations which allow time dependent inductances, is followed by specialization of these equations to tokamak applications and by the solution concept, which starts from a given time evolution of the plasma current.

In the following, the circuit equations are prepared for numerical integration by normalization, the initial values are specified and the equations which give the currents and voltages as functions of time are supplemented by the differential equations which describe the time evolution of the energies supplied to and consumed in the coils.

The next section is devoted to determination of the magnetic circuit parameters, such as self-inductances and mutual inductances, and to coefficients which describe the contributions of all coil currents to the vertical fields at the plasma centre and the inner edge of the transformer coil. All these calculations are based on an approximate solution of the Grad-Shafranov equation, which describes the magnetic flux functions produced by the various coils. The approximation mainly consists in truncating series expansion with respect to the inverse aspect ratio and harmonics of the poloidal angle after the second and third terms respectively.

In the final section the analytically calculated inductance values are compared with numerical calculations which were made for the ASDEX large divertor tokamak now being constructed at IPP. The accuracy of the inductance calculations can thus be assessed. Finally the result of a circuit calculation based on ASDEX parameters is given for illustration.

Contents

1. Introduction

A mathematical model of a tokamak fusion power plant is now being developed at IPP for the purpose of systems studies /1/. This SISYFUS computer model is aimed at taking into account the complicated relations between the various plant components as far as possible and at studying the impact of parameter variations on figures of merit (such as energy amplification, plant net efficiency), cost structures, plant layout, etc.

For use in the SISYFUS computer code a model of the pulsed magnetic circuits (plasma ring, transformer, vertical field, magnetic limiter, plasma chamber) is needed. This requirement arises from the strong impact of these circuits on plant energy balance, technology and economy. The strong bearing on the energy balance stems from the mere magnitudes of the energies and powers involved, which lead to significant losses during transfer, switching and storage. The technology aspects arise from the magnitudes of currents, voltages, fields, and energies to be handled. It is obvious that all these features finally have a strong influence on the plant economy via the cost of installation and operation.

Because of the numerous components involved it is inevitably necessary to restrict the numbers of parameters characterizing an individual component. In treating the pulsed magnetic circuits, this calls for an appraoch which emphasizes the modelling of the mutual relations but does not strive for utmost precision. This goal can be achieved by calculating the inductances and other magnetic circuit parameters from approximate solutions of the Grad-Shafranov equation describing the various poloidal field coil systems of a tokamak. As is well known for the case of the plasma ring, the simplifications are mainly due to assuming ideal toroidal symmetry and small values of the inverse aspect ratio. The errors mainly stem from extrapolating the results to appreciable values of the inverse aspect ratio. The advantage of the method lies in the possibility of characterizing each poloidal coil system by only two or three parameters.

This report is devoted to obtaining the electric circuit equations,solving them, determining the circuit parameters and describing program tests which use the ASDEX tokamak as a practical model.

All calculations use the MKSA system of units.

2. Coil system

2.1 General description of the coil arrangement

For the purpose of this paper we regard a tokamak reactor as a system of mutually coupled coils operated in a pulsed mode. We therefore do not include the toroidal field coils, which presumably will have to be superconducting and will operate in steady state. The plasma and its chamber are also treated as pulsed coils because within our context they are reduced to being current paths interlinked with time varying magnetic fields.

We restrict the coil system to be modelled to the following components:

- plasma loop (index "lp"),
- primary winding of the transformer, which induces the plasma current (index "tr"),
- vertical field windings, which provide the plasma equilibrium, and which control the position of the plasma centre (index "v"),
- magnetic limiter coils, which define the plasma edge by producing a separatrix (index "ml"),
- plasma chamber with or without poloidal slits (index "c").

Figure 1 shows schematically this system of coils with respect to the right-handed cylindrical coordinate system R, φ, z. Also shown are the currents I_{pl}, I_{tr}, I_v, I_{ml}, I_c, the inductions B_{pl}, B_{tr}, B_v, B_{ml}, B_c, and the numbers of turns (N_{tr}, N_v, N_{ml}), which are not physically unity as in the case of the plasma loop and chamber.

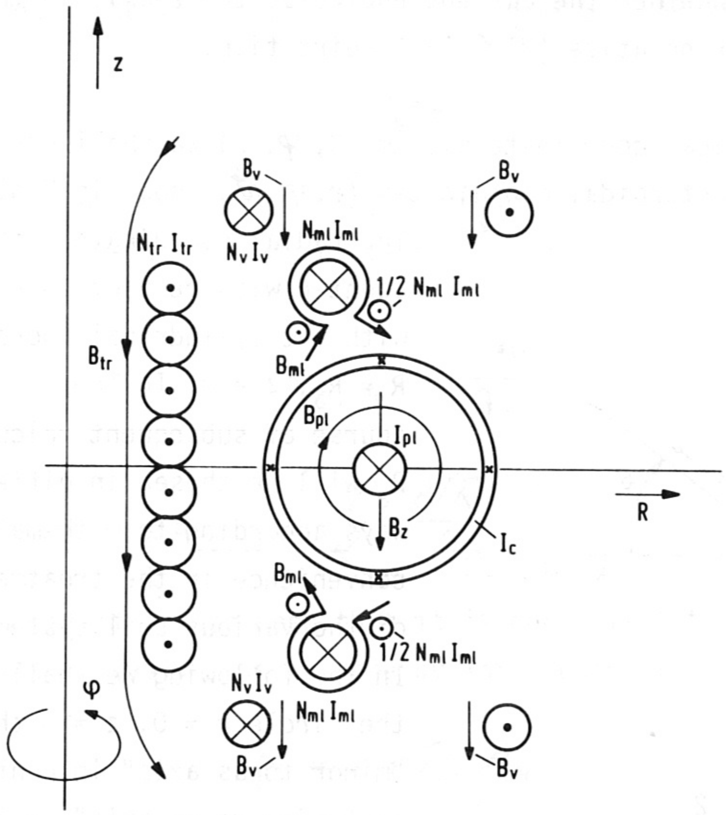

Fig. 1

2.2 Assumptions and definitions

We assume that the whole arrangement of coils is rotationally symmetric with respect to the z-axis, which means that none of the functions we use in our calculations depend on the azimuthal angle φ. This symmetry is usually called "axial symmetry" in the context of tokamaks. Furthermore we assume that all currents only have φ-components. This assumption is most important for the plasma because it implies operation at low plasma β.

Whether a current encircles the z-axis in the positive or in the negative φ-direction depends on both the winding direction and the direction of the current with respect to this winding. We therefore attribute a sign to the number N of turns to describe the winding direction and to the current I itself according to the following definition: in a winding with $N > 0$ a p o s i t i v e l y counted current flows in the positive φ-direction, whereas in a winding wich $N < 0$ a p o s i t i v e l y counted current flows in the negative φ-direction. The sign of the current is thus defined with respect to the winding direction. The sign of the product NI decides whether the current encircles the z-axis in the positive ($NI > 0$) or negative ($NI < 0$) φ-direction.

Besides the cylindrical coordinate system (R, φ, z) we shall use the so-called pseudo-toroidal coordinates (r, φ, ϑ) shown in Fig. 2.

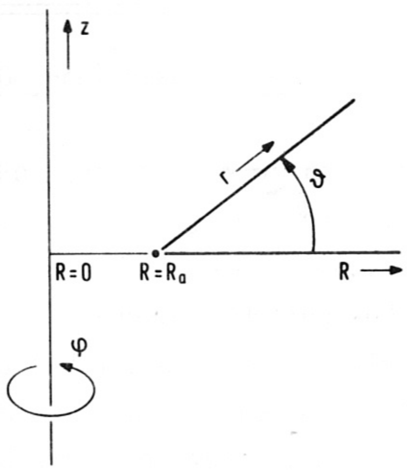

Fig. 2

The radial coordinate r is counted with respect to a point with the cylindrical coordinates $R = R_a$, $z = 0$. In the course of subsequent calculations R_a will be chosen in different ways according to mathematical convenience in the treatment of the various coil systems. In the following we shall call the circle $r = 0$, $z = 0$ the "minor torus axis" in contrast to the "major torus axis", which is identical with the z-axis.

2.3 Mathematical treatment of axially symmetric magnetic fields

In the following, we only treat poloidal magnetic fields, which are the fields produced by the currents flowing in the φ-direction. The mathematics of these fields is well known and will be repeated here only briefly for reference and to define the nomenclature.

The magnetic induction $\vec{B}_{pol}$ of the poloidal field is derived from the vector potential $\vec{A}$ by

$$\vec{B}_{pol} = \text{rot}\,\vec{A} \tag{1}$$

to satisfy Maxwell's equation

$$\text{div}\,\vec{B}_{pol} = 0 \ . \tag{2}$$

This can be done because the divergence of the toroidal induction $\vec{B}_{tor}$ vanishes separately owing to axial symmetry. Because of this symmetry the vector potential $\vec{A}$ has only a φ-component:

$$\vec{A} = A_\varphi \vec{e_\varphi} \tag{3}$$

($\vec{e_\varphi}$ = unit vector in the φ-direction). From (1) and (3) it follows that the R- and z-components of $\vec{B}_{pol}$ are

$$B_{pol,R} = -\frac{\partial A_\varphi}{\partial z}, \tag{4}$$

$$B_{pol,z} = \frac{1}{R} \cdot \frac{\partial (R A_\varphi)}{\partial R}. \tag{5}$$

From (5) it can be seen that it is convenient to use RA_φ instead of A_φ. Usually this is done by introducing the "flux function" :

$$\psi = 2\pi R . A_\varphi . \tag{6}$$

The factor 2π will be useful in interpreting ψ by means of the magnetic flux enclosed by a circular filament.

From (6), (4), and (5) one gets

$$B_{pol,\, R} = -\frac{1}{2\pi R} \cdot \frac{\partial \psi}{\partial z}, \tag{7}$$

$$B_{pol,\, z} = \frac{1}{2\pi R} \cdot \frac{\partial \psi}{\partial R}. \tag{8}$$

The two component equations (7) and (8) can be combined to form the vector equation

$$\vec{B}_{pol} = -\frac{1}{2\pi R} \cdot \vec{e_\varphi} \times grad\, \psi. \tag{9}$$

The flux function ψ follows from a partial differential equation which can easily be set up for the case of constant magnetic permeability μ.

For $\mu = \mu_0$ (μ_0 is the vacuum value of μ) one gets from

$$\vec{B} = \mu_0 \vec{H} , \tag{10}$$

$$\mathrm{rot}\, \vec{H} = \vec{j} , \tag{11}$$

with (7) and (8):

$$\mathrm{rot}\, \vec{B}_{pol} = \frac{1}{2\pi} \left[-\frac{1}{R} \cdot \frac{\partial^2 \psi}{\partial z^2} - \frac{\partial}{\partial R} \left(\frac{1}{R} \cdot \frac{\partial \psi}{\partial R} \right) \right] \vec{e}_\varphi = \mu_0 j_\varphi \vec{e}_\varphi \tag{12}$$

(j_φ = toroidal current density). Equation (12) leads to

$$\frac{\partial^2 \psi}{\partial R^2} - \frac{1}{R} \frac{\partial \psi}{\partial R} + \frac{\partial^2 \psi}{\partial z^2} = -2\pi \mu_0 R j_\varphi . \tag{13}$$

Equation (13) allows the ψ-field to be determined if its sources (the spatial distribution of j_φ) and appropriate boundary conditions for ψ are specified.

In any plane φ = const the lines defined by ψ = const coincide with the field lines of $\vec{B}_{pol}$. This is due to

$$\vec{B}_{pol} \cdot \mathrm{grad}\, \psi = 0 , \tag{14}$$

which follows directly from (9). Equation (14) states that $\vec{B}_{pol}$ is normal to grad ψ and hence parallel to the lines ψ = const.

Being rotated around the z-axis, the lines ψ= const sweep the so-called magnetic surfaces. For the special case of a toroidal plasma in ideal MHD equilibrium these magnetic surfaces have to be normal to the gradient of the plasma pressure p because of the condition

$$\mathrm{grad}\; p = \vec{j} \times \vec{B} \tag{15}$$

Thus the lines ψ = const in any cross-section φ= const are also lines p = const.

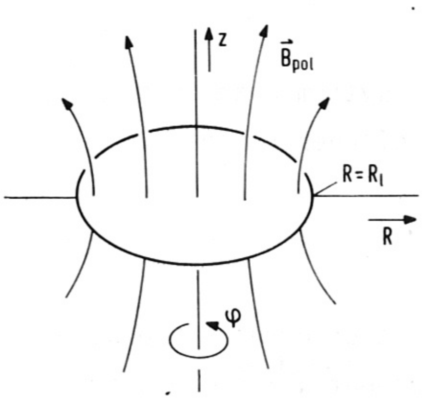

Fig. 3

The flux function ψ and the poloidal magnetic flux ϕ_{pol} are closely connected. This can be demonstrated by calculating the flux ϕ_{pol} which penetrates the circular loop $R = R_\ell$, $z = 0$ shown in Fig. 3. This flux ϕ_{pol} is given by

$$\phi_{pol} = \iint_F \overrightarrow{B_{pol}} \cdot \overrightarrow{dF} . \tag{16}$$

By inserting (9) and

$$dF = RdRd\varphi . \vec{e}_z \tag{17}$$

in (16) one gets

$$\phi_{pol} = \int_0^{R_\ell} grad_R \psi . dR = \psi(R_\ell) - \psi(0). \tag{18}$$

Because ϕ_{pol} becomes zero for $R_\ell \to \infty$ one gets

$$\psi(\infty) = \psi(0). \tag{19}$$

From (18) and (19) follows

$$\phi_{pol} = \psi(R_\ell) - \psi(\infty) . \tag{20}$$

2.4 Magnetic energy

If the vector potential of a magnetic system changes by $\delta\vec{A}$ this is associated by the following change of energy density:

$$\delta e = \vec{j} \cdot \delta\vec{A} . \tag{21}$$

This variation δ_e is made up by changes in the currents producing $\vec{A}$ and by variations of the geometrical arrangement which may occur.

Equation (21) is valid if no polarization of matter has to be accounted for (this means $\mu = \mu_0$) and can easily be transformed to the well-known formulation

$$\delta e = \vec{H} \cdot \delta\vec{B} \tag{22}$$

by using $\vec{j} = \mathrm{rot}\, \vec{H}$ together with the rapid spatial decay of $\delta\vec{A} \times \vec{H}$. The latter is due to the dipole character of magnetic fields produced by electric currents which are constrained to finite volumes.

Generally δe is not a total differential because of the polarization omitted.

An important exception is when $\vec{B}$ is strictly proportional to $\vec{H}$:

$$\vec{B} = \mu_r \mu_0 \vec{H} \tag{23}$$

(μ_0 = permeability of the vacuum, μ_r = const = relative permeability). Equation (23) is valid for the vacuum (μ_r = 1) and for all substances which display an induced dipole moment proportional to $\vec{H}$. By inserting $\vec{B}$ from (23) into (22) and integrating over the volume V we get the total stored magnetic energy

$$E_m = \frac{1}{2} \int_V \vec{H} \cdot \vec{B} \, dV . \tag{24}$$

The corresponding formula for E_m in terms of $\vec{j}$ and $\vec{A}$ is

$$E_m = \frac{1}{2} \int_V \vec{j} \cdot \vec{A} \, dV . \tag{25}$$

For our special case of the poloidal field (25) reduces to

$$E_m = \frac{1}{2}\int_V j_\varphi A_\varphi \, dV \tag{26}$$

$$= \frac{1}{4\pi}\int_V \frac{1}{R}\psi j_\varphi \, dV. \tag{27}$$

Equations (26) or (27) can be used for calculating the stored magnetic energy E_{jk} due to the interaction of two coil systems "j" and "k". With $A_{\varphi j}$, ψ_j, and $A_{\varphi k}$, ψ_k being the vector potentials and flux functions produced by the current densities $j_{\varphi j}$ and $j_{\varphi k}$ respectively, one gets from (26) and (27)

$$E_{jk} = \frac{1}{2}\int_V j_{\varphi j} A_{\varphi k} \cdot dV = \frac{1}{2}\int_V j_{\varphi k} A_{\varphi j} \cdot dV. \tag{28}$$

This is equivalent to

$$E_{jk} = \frac{1}{4\pi}\int_V \frac{1}{R} j_{\varphi j} \psi_k \cdot dV = \frac{1}{4\pi}\int_V \frac{1}{R} j_{\varphi k} \psi_j \cdot dV. \tag{29}$$

E_{jk} is the stored magnetic energy due to the interaction of the vector potential $A_{\varphi k}$ (produced by $j_{\varphi k}$) with the current density $j_{\varphi j}$, E_{kj} is the magnetic energy corresponding to the reverse interaction.

The total stored energy E_m is given by

$$E_m = E_{jk} + E_{kj} = 2E_{jk} \, . \tag{30}$$

The energies obey the symmetry relation

$$E_{jk} = E_{kj} \tag{31}$$

which can be derived on the basis of the vector potential $\vec{A}$. Equation (31) has already been used in (28), (29), and (30).

3. Electric circuit

3.1 General equations for magnetically coupled coils

All coils of our system are mutually coupled by magnetic fields. This is shown schematically in Fig. 4. The coupling is quantified by the mutual inductances M_{jk} between the coils "j" and the coils "k". A current I_k flowing in coil k produces a magnetic field which interacts with the current I_j flowing in coil "j". The corresponding energy of interaction E_{jk} is written as

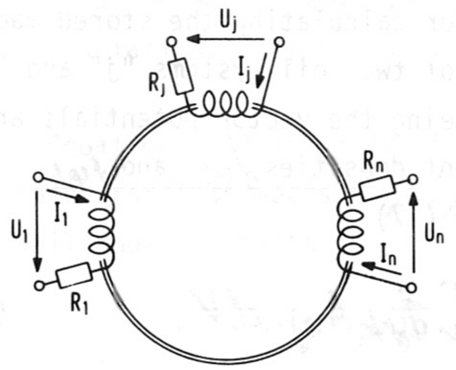

Fig. 4

$$E_{jk} = \frac{1}{2} M_{jk} I_j I_k \quad . \tag{32}$$

The energy E_{kj} of the reverse interaction is given by

$$E_{kj} = \frac{1}{2} M_{kj} I_j I_k \quad . \tag{33}$$

The mutual inductance M_{jk} can be determined by using the field theory result for E_{jk} given by (28). For M_{jk}, for instance, one gets

$$M_{jk} = \frac{1}{I_j I_k} \int_V j_{\varphi j} A_{\varphi k} \, dV. \tag{34}$$

The vector potential $A_{\varphi k}$ is a functional of $j_{\varphi k}$ and of the geometry. The dependence is always of such a kind that M_{jk} is invariant with respect to interchanging j and k. This symmetry relation

$$M_{jk} = M_{kj} \tag{35}$$

follows from (31).

The currents I_j and I_k which result from integrating $\dot{j}_{\varphi j}$ and $\dot{j}_{\varphi k}$ over the conductor cross-sections disappear from (34) in actual calculations if the distributions of $\dot{j}_{\varphi j}$ and $\dot{j}_{\varphi k}$ over these cross-sections are fixed. There may be a certain arbitrariness in calculating I_j and I_k if they result from continuous current distributions such as pertain to, for example, the plasma chamber. In such cases, the I_j's and I_k's are defined as integrals over certain cross--sectional domains which can be chosen according to mathematical convenience. Once these domains have been chosen, however, they have to be used consistently for all calculations which involve I_j and I_k, as, for example, the determination of M_{jk} from (34).

To derive the circuit equations, we consider the energies exchanged between an energy source j, the coil system j and the resistor R_j (see Fig. 4).

The electric energy δE_{ej} delivered by the source is given by

$$\delta E_{ej} = U_j\, \delta Q_j = U_j\, I_j\, \delta t \tag{36}$$

where δQ_j is the electric charge entering the system.

The corresponding energy variation δE_j of the coil system follows from (21) by volume integration:

$$\delta E_j = \int_V \vec{j} \cdot \delta\vec{A}\, dV. \tag{37}$$

The equivalent to (37) in terms of circuit parameters is

$$\delta E_j = \sum_{k=1}^{n} I_j\, \delta(M_{jk} I_k). \tag{38}$$

The sum (38) has to extend over all coils of the system because of their interaction with coil j. The energy variation δE_{rj} due to dissipation in the resistor R_j follows from

$$\delta E_{rj} = U_{rj}\, \delta Q_j\, . \tag{39}$$

With the resistive voltage drop

$$U_{rj} = I_j R_j \tag{40}$$

and $\delta Q_j = I_j \delta t$ we get from (39)

$$\delta E_{rj} = I_j^2 R_j \delta t . \tag{41}$$

Up to now the energy variations $\delta E_{ej}, \delta E_j$ and δE_{rj} have been treated as uncorrelated. In fact, they have to obey the energy balance

$$\delta E_{ej} = \delta E_j + \delta E_{rj} . \tag{42}$$

By inserting (36), (38), and (41) in (42) we get

$$\sum_{k=1}^{n} \delta(M_{jk} I_k) + I_j R_j \delta t = U_j \delta t . \tag{43}$$

The variation $\delta(M_{jk} I_k)$ is given by

$$\delta(M_{jk} I_k) = \frac{d(M_{jk} I_k)}{dt} \delta t . \tag{44}$$

Equation (44) inserted in (43) leads to the circuit equation

$$\sum_{k=1}^{n} (M_{jk} I_k)^{\dot{}} + R_j I_j = U_j \tag{45}$$

(the dot means differentiation with respect to t).

Because the above derivation applies to each of the n coils equation (45) is valid for j = 1, 2, ... n, which means that we have n equations to correlate the voltages U_j with I_j and $\dot{I}_j$.

The set (45) of circuit equations was derived within a framework of energy exchange. This shows that (45) is not restricted to filamentary current loops interlinked with magnetic fluxes but also applies to the magnetic interaction of spatially distributed currents. Obviously, these current distributions have to be reasonable within the framework of magnetic circuits, which means that it must be possible to define closed currents by integrals over appropriately chosen cross-sections. The plasma current and the current induced in the plasma chamber are of this kind. Equations (45) allow the case of M_{jk}'s varying with time to be treated. This is an important feature for our application, where the plasma major and minor radii may vary with time, thus causing variations of the inductances.

3.2 Specialization to the poloidal field system of a tokamak

We now specialize the circuit equations (45) to the poloidal field coil system of the tokamak described in Section 2.1.

To avoid complicated indexing in the circuit equations the coils and corresponding currents and voltages in this section are numbered according to the following scheme:

plasma	pl	1
transformer	tr	2
vertical field	v	3
magnetic limiter	ml	4
chamber, mean value	c0	5
chamber, dipole component	c1	6
chamber, quadrupole component	c2	7

The chamber current has been subdivided into three components I_{c0}, I_{c1}, I_{c2} (here named I_5, I_6, I_7), which takes into account the fact that the chamber current density $j_{c\varphi}$ depends on the poloidal angle ϑ owing to toroidal curvature. The three components emerge from a Fourier expansion truncated after the third term of the current I_c which results from integrating $j_{c\varphi}$ over the chamber cross-section (see section 5.4.4).

The transformer, the vertical field coils and the magnetic limiter coils are powered by energy sources with voltages U_{tr}, U_v, and U_{ml} (here named U_2, U_3, and U_4).

All coils have ohmic resistances R_i. The plasma resistance $R_1(t)$ will, in general, be a function of time and will be given as input (see Section 3.3). The remaining resistances will either be given as input or calculated from input data.

3.3 Compilation of the equations to be used

The coils, currents, voltages, and resistances are schematically visualized in Fig. 5. The corresponding circuit equations based on the general form (45) are

$$(L_1 I_1)^{\cdot} + \sum_{k=2}^{7} (M_{1k} I_k)^{\cdot} + I_1 R_1(t) = 0\,, \tag{46}$$

$$(L_2 I_2)^{\cdot} + \sum_{k=1}^{7}{}_{\neq 2} (M_{2k} I_k)^{\cdot} + I_2 R_2 = U_2\,, \tag{47}$$

$$(L_3 I_3)^{\cdot} + \sum_{k=1}^{7}{}_{\neq 3} (M_{3k} I_k)^{\cdot} + I_3 R_3 = U_3\,, \tag{48}$$

$$(L_4 I_4)^{\cdot} + \sum_{k=1}^{7}{}_{\neq 4} (M_{4k} I_k)^{\cdot} + I_4 R_4 = U_4\,, \tag{49}$$

$$(L_5 I_5)^{\cdot} + \sum_{k=1}^{7}{}_{\neq 5} (M_{5k} I_k)^{\cdot} + I_5 R_5 = 0\,, \tag{50}$$

$$(L_6 I_6)^{\cdot} + \sum_{k=1}^{7}{}_{\neq 6} (M_{6k} I_k)^{\cdot} + I_6 R_6 = 0\,, \tag{51}$$

$$(L_7 I_7)^{\cdot} + \sum_{k=1}^{6} (M_{7k} I_k)^{\cdot} + I_7 R_7 = 0\,. \tag{52}$$

When going from (45) to (46) - (52) we have introduced the usual nomenclature

$$L_j = M_{jj}. \tag{53}$$

L_j is the self-inductance, the value of the mutual inductance M_{jk} for the special case j = k.

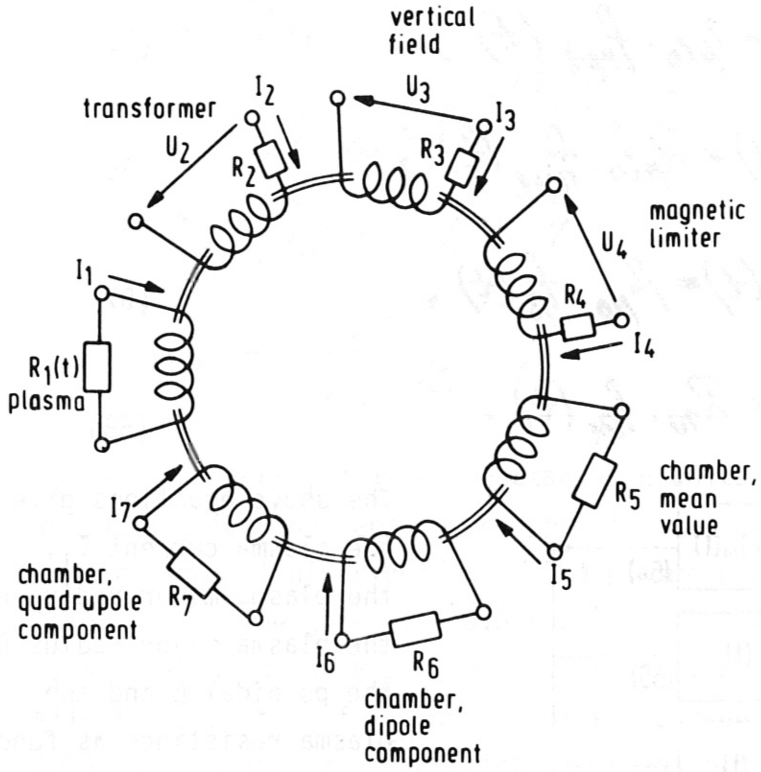

Fig. 5

We shall not use (46) to (52) to calculate the currents I_j for given voltages U_j but to determine the voltages which correspond to a plasma current prescribed as a function of time. This procedure accounts for the fact that the plasma is the most sensitive component of the system and therefore, in general, calls for a certain kind of time history. Because the plasma has to be maintained in equilibrium and its boundary is assumed to be defined by a separatrix, prescription of the plasma current has to be supplemented by specification of the plasma position, plasma shape and plasma dimensions. This, in turn, imposes conditions on the variation of vertical field and magnetic limiter currents with time.

We shall now describe the procedure which leads from the given information to determination of all currents and voltages involved. The scheme is shown in Fig. 6 (the small numbers designate the equations used).

The procedure starts from

$$I_1 = I_1(t) = I_{10} \cdot f_{I1}(t) , \tag{54}$$

$$r_{pl} = r_{pl}(t) = r_{plo} \cdot f_{rpl}(t) , \tag{55}$$

$$R_{pl} = R_{pl}(t) = R_{plo} \cdot f_{Rpl}(t) , \tag{56}$$

$$\beta_{pol} = \beta_{pol}(t) = \beta_{po} \cdot f_{\beta}(t) , \tag{57}$$

$$R_1 = R_1(t) = R_{10} \cdot f_{R1}(t) . \tag{58}$$

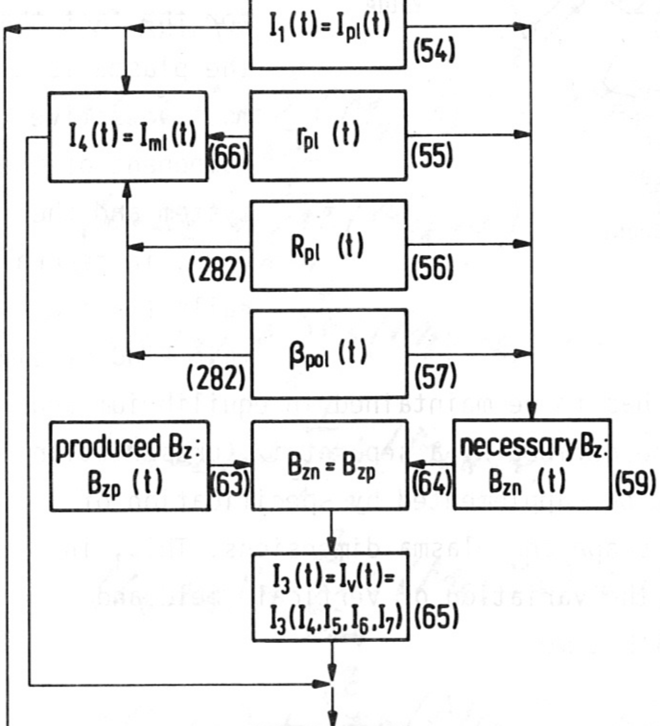

Fig. 6

The above equations give the plasma current I_1, the plasma minor radius r_{pl}, the plasma major radius R_{pl}, the poloidal β and the plasma resistance as functions of time. I_{10}, r_{plo}, R_{plo}, β_{po}, and R_{10} are normalization values introduced to keep the functions $f_{I1}(t)$, $f_{rp1}(t)$, $f_{Rp1}(t)$, $f_{\beta}(t)$, and $f_{R1}(t)$ of order unity. These functions will, in general, emerge from calculations with a computer program modelling plasma performance such as the NUDIPLAS /2/ or WHIST codes.

We shall assume that the plasma minor cross-section will be of circular shape, as has already been tacitly done. When introducing the plasma minor radius r_{pl}. For this case the vertical magnetic field B_z at $R = R_{pl}$, $z = 0$ n e c e s s a r y for plasma equilibrium is given by /3/

$$B_z = B_{zn} = \nu I_1 \tag{59}$$

with
$$\nu = -\frac{\mu_0}{4\pi R_{pl}} \left(\ln \frac{8 R_{pl}}{r_{pl}} + \lambda_1 - 1/2 \right), \tag{60}$$

$$\lambda_1 = \beta_{pol} + l_i/2 - 1, \tag{61}$$

$$l_i = \frac{L_{pl,i}}{\mu_0 R_{pl}/2} \; ; \tag{62}$$

l_i is the internal plasma inductance in units of $\mu_0 R_{pl}/2$, which is twice the zero-order approximation for l_i in the case of a uniform spatial distribution of the plasma current density. Accordingly, one gets $l_i = 0{,}5$ for a uniform current distribution; $l_i = 1$ is valid for a parabolic distribution. There is therefore a slight dependence of B_{zn} on the plasma current profile. Equations (59) to (62) are the transcription of equation (37) in /3/ to MKSA units and our coordinate system (Fig. 2).

The vertical field B_z contains contributions from the currents flowing in the various coils, as is expressed by the following formula for the p r o d u c e d vertical field B_z:

$$B_{zp} = \nu_3 I_3 + \nu_4 I_4 + \nu_5 I_5 + \nu_6 I_6 + \nu_7 I_7 \, . \tag{63}$$

The transformer current is assumed to produce no contribution to B_z $(\nu_2 = 0)$, The parameters ν depend on the position of the coils relative to the plasma centre. The determination of the ν will be described in Section 5.7.

By using

$$B_{zp} = B_{zn} \tag{64}$$

we get from (63) an equation which gives the necessary vertical field current I_3 as a function of the plasma current I_1, the magnetic limiter current I_4 and the chamber currents I_5, I_6, and I_7:

$$I_3 = \frac{1}{\nu_3}\left(\nu I_1 - \nu_4 I_4 - \nu_5 I_5 - \nu_6 I_6 - \nu_7 I_7\right) \quad (65)$$

To eliminate the magnetic limiter current I_4 from (65), we use the fact that I_4 is proportional to the plasma current. The factor f of proportionality depends on the plasma major and minor radii, on ß as well as on the positions of the stagnation point and the multipole windings. From

$$I_4 = f \cdot I_1 \quad (66)$$

and (54) we get

$$I_4 = I_{10} \cdot f_{I4} \quad (67)$$

with

$$f_{I4} = f_{I1} \cdot f. \quad (68).$$

In Section 5.9 we shall give a formula for calculating f. By inserting (66) into (65) we get I_3 in terms of the plasma current and the chamber currents:

$$I_3 = \frac{1}{\nu_3}\left(\nu I_1 - \nu_4 f I_1 - \nu_5 I_5 - \nu_6 I_6 - \nu_7 I_7\right). \quad (69)$$

Up to now we have not used circuit equations out of the set (46) to (52) but have determined I_1, I_3 and I_4 in terms of input data and the chamber currents I_5, I_6, and I_7. To calculate I_5, I_6, I_7 and the transformer current I_2, we use (46), (50), (51),and (52) out of the complete set of circuit equations, supplemented by I_1, I_3, and I_4 according to (54), (69), and (66). We thus have to solve a system of four coupled, linear first-order differential equations. This can be done either by directly solving the complete system or by an iteration procedure.

From (46) we get for $(M_{12}I_2)^{\cdot}$

$$(M_{12} I_2)^{\cdot} = -(L_1 I_1 + M_{13} I_3 + M_{14} I_4 + M_{15} I_5 + M_{16} I_6 + M_{17} I_7)^{\cdot} - I_1 R_1 . \qquad (70)$$

The chamber currents I_4, I_5, and I_6 influence I_2 explicitely and via I_3 according to (69). In any calculation of I_2 from now on we shall treat I_5, I_6, and I_7 as given by a previous calculation. In the first step we set I_4, I_5, and I_6 equal to zero.

For I_4, I_5, and I_6 we get from (50) to (52)

$$L_5 \dot{I}_5 + M_{56} \dot{I}_6 + M_{57} \dot{I}_7 + R_5 I_5 = \dot{F}_{u5} , \qquad (71)$$

$$M_{56} \dot{I}_5 + L_6 \dot{I}_6 + M_{67} \dot{I}_7 + R_6 I_6 = \dot{F}_{u6} , \qquad (72)$$

$$M_{57} \dot{I}_5 + M_{67} \dot{I}_6 + L_7 \dot{I}_7 + R_7 I_7 = \dot{F}_{u7} \qquad (73)$$

with

$$\dot{F}_{u5} = -(M_{51} I_1 + M_{52} I_2 + M_{53} I_3 + M_{54} I_4)^{\cdot} , \qquad (74)$$

$$\dot{F}_{u6} = -(M_{61} I_1 + M_{62} I_2 + M_{63} I_3 + M_{64} I_4)^{\cdot} , \qquad (75)$$

$$\dot{F}_{u7} = -(M_{71} I_1 + M_{72} I_2 + M_{73} I_3 + M_{74} I_4)^{\cdot} . \qquad (76)$$

Here we have used the fact that all inductances of the chamber (L_5, L_6, L_7, M_{56}, M_{57}, M_{67}) do not vary with time because of the rigid geometry. The right-hand sides $\dot{F}_{u5}$ to $\dot{F}_{u7}$ are given functions of time because of (54), (70), (65), and (66) if we treat I_5 to I_7 as described above. We thus get I_5 to I_7 from the iterative solution of (71) to (73) and finally I_3 from (69).

Up to this point the three equations (47), (48), and (49) have not been used. They now serve to determine the voltages U_2, U_3, and U_4 necessary to drive the prescribed plasma and magnetic limiter currents (I_1 and I_4) together with the necessary transformer and vertical field currents (I_2 and I_3) and the currents induced in the chamber walls (I_5, I_6, and I_7).

4. Solution of the circuit equations

4.1 Initial conditions for the currents

We choose $t = t_o$ as starting time of the calculation. The values of the currents I_1 to I_7 for $t = t_o$ are

$$I_1(t_o) = I_{10} \cdot f_{I_1}(t_o) \,, \tag{77}$$

$$I_2(t_o) \,, \tag{78}$$

$$I_3(t_o) = \frac{1}{v_3}\left[v(t_o) I_1(t_o) - v_4 I_4(t_o)\right] , \tag{79}$$

$$I_4(t_o) = I_1(t_o) \cdot f(t_o) \,, \tag{80}$$

$$I_5(t_o) = 0 \,, \tag{81}$$

$$I_6(t_o) = 0 \,, \tag{82}$$

$$I_7(t_o) = 0 \,. \tag{83}$$

Equation (77) follows from the given plasma current distribution (54). $I_2(t_o)$ is an input parameter. In general, $I_2(t_o)$ will be chosen such that a symmetric magnetic flux swing during one burn pulse results. $I_3(t_o)$ follows from (77) and (80) to (83); $v(t_o)$ is calculated from (60) by using $R_{pl}(t_o)$, $r_{pl}(t_o)$, and $\beta_{pol}(t_o)$, which are input data. $I_4(t_o)$ follows from (66) for $t = t_o$. $I_5(t_o) = I_6(t_o) = I_7(t_o) = 0$ describes the assumption that chamber currents induced during a previous burn pulse have already completely decayed at the beginning of the pulse considered.

4.2 Normalizations

We introduce two characteristic times τ_h and τ_6 :

- τ_h is a time inverval characteristic of major plasma current changes such as the current build-up time.

- τ_b is a time interval of the order of the burn pulse length. It will later be used for the normalization of energies.

In the differential equations we normalize t to τ_h:

$$t^* = t/\tau_h \, , \tag{84}$$

$$d/dt^* = \tau_h \cdot d/dt \, . \tag{85}$$

In all subsequent normalized equations " · " means differentiation with respect to t^* !

The currents I_1 to I_7 are normalized according to the following scheme:

$$\begin{aligned} y_1 &= I_1/I_{10} \, , \\ y_2 &= I_2/I_{20} \, , \\ y_3 &= I_3/I_{10} \, , \\ y_4 &= I_4/I_{10} \, , \\ y_5 &= I_5/I_{50} \, , \\ y_6 &= I_6/I_{50} \, , \\ y_7 &= I_7/I_{50} \, . \end{aligned} \tag{86}$$

I_{10} is the normalization value for the plasma current introduced by (54).

I_{20} and I_{50} give the order of the transformer and chamber currents due to varying plasma current:

$$I_{20} = \frac{L_{10}}{M_{120}} I_{10} \, , \tag{87}$$

$$I_{50} = \frac{M_{150}}{R_c} \cdot \frac{I_{10}}{\tau_h} \, . \tag{88}$$

The choice of I_{20} reflects the fact that the transformer voltage drop for rapid plasma current changes is mainly inductive.

I_{50} emerges from the assumption that the chamber voltage drop is mainly resistive.

L_{10}, M_{120}, and M_{150} are the inductances L_1, M_{12}, and M_{15} calculated for

$$L_{10} = L_1(r_{pl0}, R_{pl0}), \tag{89}$$

$$M_{120} = M_{12}(r_{pl0}, R_{pl0}), \tag{90}$$

$$M_{150} = M_{15}(r_{pl0}, R_{pl0}). \tag{91}$$

R_c is the ohmic resistance of the chamber the long way round if no poloidal slit is present.

4.3 Normalized differential equations for the currents

We solve (71) to (73) for I_5, I_6, and I_7. The result is

$$\dot{I}_5 = A_{55} I_5 + A_{56} I_6 + A_{57} I_7 + \dot{H}_5, \tag{92}$$

$$\dot{I}_6 = A_{65} I_5 + A_{66} I_6 + A_{67} I_7 + \dot{H}_6, \tag{93}$$

$$\dot{I}_7 = A_{75} I_5 + A_{76} I_6 + A_{77} I_7 + \dot{H}_7 \tag{94}$$

with the coefficients A_{mn} given by

$$\begin{aligned} A_{55} &= -L_6 L_7 (1-k_{67}^2) R_5/D, & A_{65} &= M_{56} L_7 R_5/D, \\ A_{56} &= M_{56} L_7 R_6/D, & A_{66} &= -L_5 L_7 R_6/D, \\ A_{57} &= M_{56} M_{67} R_7/D, & A_{67} &= -L_5 M_{67} R_7/D, \\ A_{75} &= M_{56} M_{67} R_5/D, \\ A_{76} &= L_5 M_{67} R_6/D, \\ A_{77} &= L_5 L_6 (1-k_{56}^2) R_7/D; \end{aligned} \tag{95}$$

$$\mathcal{D} = L_5 L_6 L_7 (1 - k_{56}^2 - k_{67}^2),$$
$$k_{56}^2 = M_{56}^2 / L_5 L_6 , \qquad (96)$$
$$k_{67}^2 = M_{67}^2 / L_6 L_7 .$$

In the calculation of the A_{mn} we have already used the special result $M_{57} = M_{75} = 0$, which is due to the approximate method of determining the inductances (see Section 5.5.7). The A_{mn} do not possess a symmetry property. It should therefore be borne in mind that

$$A_{mn} \neq A_{nm} . \qquad (97)$$

The functions $\dot{H}_5$, $\dot{H}_6$, and $\dot{H}_7$ are given by

$$\dot{H}_5 = [L_6 L_7 (1 - k_{67}^2) \dot{F}_{n5} - M_{56} L_7 \dot{F}_{n6} + M_{56} M_{67} \dot{F}_{n7}] / \mathcal{D} ,$$
$$\dot{H}_6 = [-M_{56} L_7 \dot{F}_{n5} + L_5 L_7 \dot{F}_{n6} - L_5 M_{67} \dot{F}_{n7}] / \mathcal{D} , \qquad (98)$$
$$\dot{H}_7 = [M_{56} M_{67} \dot{F}_{n5} - L_5 M_{67} \dot{F}_{n6} + L_5 L_6 (1 - k_{56}^2) \dot{F}_{n7}] / \mathcal{D} .$$

Normalization of $\dot{H}_5$, $\dot{H}_6$, and $\dot{H}_7$ to I_{50} and τ_n yields

$$h_5 = \frac{d}{dt^*} (H_5 / I_{50}) = \tau_n \dot{H}_5 / I_{50} ,$$
$$h_6 = \frac{d}{dt^*} (H_6 / I_{50}) = \tau_n \dot{H}_6 / I_{50} , \qquad (99)$$
$$h_7 = \frac{d}{dt^*} (H_7 / I_{50}) = \tau_n \dot{H}_7 / I_{50} .$$

The orders of L/R-times are given by

$$\tau_5 = - 1/A_{55} = \frac{1 - k_{56}^2 - k_{67}^2}{1 - k_{67}^2} \cdot \frac{L_5}{R_5} ,$$
$$\tau_6 = - 1/A_{66} = (1 - k_{56}^2 - k_{67}^2) \cdot \frac{L_6}{R_6} , \qquad (100)$$
$$\tau_7 = - 1/A_{77} = \frac{1 - k_{56}^2 - k_{67}^2}{1 - k_{56}^2} \cdot \frac{L_7}{R_7} .$$

By introducing y_5, y_6, y_7 according to (86) together with (99) and (100) into (92, (93), and (94) we get the following normalized differential equations for y_5 to y_7 :

$$\dot{y}_5 = -\frac{\tau_n}{\tau_5}\left(y_5 + \frac{A_{56}}{A_{55}} y_6 + \frac{A_{57}}{A_{55}} y_7 + \dot{h}_5\right), \qquad (101)$$

$$\dot{y}_6 = -\frac{\tau_n}{\tau_6}\left(\frac{A_{65}}{A_{66}} y_5 + y_6 + \frac{A_{67}}{A_{66}} y_7 + \dot{h}_6\right), \qquad (102)$$

$$\dot{y}_7 = -\frac{\tau_n}{\tau_7}\left(\frac{A_{75}}{A_{77}} y_5 + \frac{A_{76}}{A_{77}} y_6 + y_7 + \dot{h}_7\right). \qquad (103)$$

If we treat a chamber which prevents a toroidal current I_5 by means of a poloidal slit, we only have to set $y_5 \equiv 0$ and solve (102), (103) with the terms containing y_5 omitted (formally a poloidal slit leads to $R_5 \rightarrow \infty$).

The functions $\dot{h}_5$, $\dot{h}_6$, and $\dot{h}_7$ depend on I_1 to I_4 via $\dot{F}_{h5}$, $\dot{F}_{h6}$ and $\dot{F}_{h7}$, which means that they depend on $\dot{y}_1$ to $\dot{y}_4$. We shall not write down here $\dot{h}_5$ to $\dot{h}_7$ in terms of $\dot{y}_1$ to $\dot{y}_4$ but shall only give the equations for y_1 to y_4 :

$$y_1 = f_{I1}(t^*), \qquad (104)$$

$$y_2 = y_2(t_0^*) - \frac{M_{120}}{M_{12}}\left\{\frac{L_1}{L_{10}}\left[y_1 - y_1(t_0^*)\right] + \frac{M_{13}}{L_{10}}\left[y_3 - y_3(t_0^*)\right] + \frac{M_{14}}{L_{10}}\left[y_4 - y_4(t_0^*)\right] + \frac{M_{15} M_{150}}{L_{10}\tau_n R_c} y_5 + \frac{M_{16} M_{150}}{L_{10}\tau_n R_c} y_6 + \frac{M_{17} M_{150}}{L_{10}\tau_n R_c} y_7\right\} - \frac{\tau_n M_{120} R_{10}}{L_{10} M_{12}} \int_{t_0^*}^{t^*} f_{I2} f_{R1}\, dt^*, \qquad (105)$$

$$y_3 = \frac{1}{U_3}\left(U - U_4 - U_5 \frac{M_{150}}{\tau_n R_c} y_5 - U_6 \frac{M_{150}}{\tau_n R_c} y_6 - \frac{M_{150}}{\tau_n R_c} y_7\right), \qquad (106)$$

$$y_4 = f_{I4}(t^*). \qquad (107)$$

y_1 according to (104) is the normalized form of (66) transferred to the t^*-scale.

y_2 according to (105) results from the integration over t^* of the normalized form of (70). The initial conditions (77) to (83) have been accounted for in normalized form.

y_3 according to (106) is the normalized form of (69) transferred to the t^*-scale.

y_4 according to (107) is the normalized form of (67) transferred to the t^*-scale.

The set of equations (101) to (107) can be solved by any numerical integration procedure and yields $y_2(t^*)$, $y_3(t^*)$, $y_5(t^*)$, $y_6(t^*)$, and $y_7(t^*)$. The currents y_1 and y_4 are input functions. The voltages U_2 to U_4 follow from inserting the dy/dt^* into (47) to (49), taking into account the normalizations of currents and time.

4.4 Normalized differential equations for the electric energies

During one cycle of tokamak operation the power supplies "2", "3", "4" with the voltages U_2 (transformer), U_3 (vertical field), and U_4 (magnetic limiter) shown in Fig. 5 deliver energy to (or get energy back from) the coil system. Part of the energy supplied is dissipated in the various coils. We calculate the following energies as functions of time:

E_1 . . . energy supplied by the transformer power supply,
E_2 . . . energy supplied by the vertical field power supply,
E_3 . . . energy supplied by the magnetic limiter power supply,
E_4 . . . energy dissipated in the plasma,
E_5 . . . energy dissipated in the transformer windings,
E_6 . . . energy dissipated in the vertical field windings,
E_7 . . . energy dissipated in the magnetic limiter windings,
E_8 . . . energy dissipated by chamber current I_5,
E_9 . . . energy dissipated by chamber current I_6,
E_{10} . . energy dissipated by chamber current I_7.

We normalize the energies E_1 to E_{10} according to the following scheme:

$$e_1 = E_1 / \tfrac{1}{2} L_{10} I_{10}^2 , \tag{108}$$

$$e_2 = E_2 / \tfrac{1}{2} L_{30} I_{10}^2 , \tag{109}$$

$$e_3 = E_3 / \tfrac{1}{2} L_{40} I_{10}^2 , \tag{110}$$

$$e_4 = E_4 / I_{10}^2 R_{10} \tau_6 \,, \tag{111}$$

$$e_5 = E_5 / I_{20}^2 R_2 \tau_6 \,, \tag{112}$$

$$e_6 = E_6 / I_{10}^2 R_3 \tau_6 \,, \tag{113}$$

$$e_7 = E_7 / I_{10}^2 R_4 \tau_6 \,, \tag{114}$$

$$e_8 = E_8 / I_{60}^2 R_5 \tau_6 \,, \tag{115}$$

$$e_9 = E_9 / I_{50}^2 R_6 \tau_6 \,, \tag{116}$$

$$e_{10} = E_{10} / I_{50}^2 R_7 \tau_6 \,. \tag{117}$$

The normalized energies are determined from the following equations, which represent the normalized powers de/dt*:

$$\frac{de_1}{dt^*} = \frac{2\tau_h}{L_{10} I_{10}^2} u_2 I_2 \,, \tag{118}$$

$$\frac{de_2}{dt^*} = \frac{2\tau_h}{L_{30} I_{10}^2} u_3 I_3 \,, \tag{119}$$

$$\frac{de_3}{dt^*} = \frac{2\tau_h}{L_{40} I_{10}^2} u_4 I_4 \,, \tag{120}$$

$$\frac{de_4}{dt^*} = f_{R1} \frac{\tau_h}{\tau_6} y_1^2 \,, \tag{121}$$

$$\frac{de_5}{dt^*} = \frac{\tau_h}{\tau_6} y_2^2 \,, \tag{122}$$

$$\frac{de_6}{dt^*} = \frac{\tau_h}{\tau_6} y_3^2 \,, \tag{123}$$

$$\frac{de_7}{dt^*} = \frac{\tau_h}{\tau_6} y_4^2 \,, \tag{124}$$

$$\frac{de_8}{dt^*} = \frac{\tau_h}{\tau_6} y_5^2 \quad , \tag{125}$$

$$\frac{de_9}{dt^*} = \frac{\tau_h}{\tau_6} y_6^2 \quad , \tag{126}$$

$$\frac{de_{10}}{dt^*} = \frac{\tau_h}{\tau_6} y_7^2 \quad . \tag{127}$$

The differential equations (118) to (127) are integrated numerically with the initial conditions

$$e_i(t_0^*) = 0 \quad ; \quad i = 1, \ldots 10 \tag{128}$$

which means that we count the energies from the starting time t_0 of the calculation.

In practice, the energy equations (128) to (127) are solved simultaneously with the current equations (101) to (107), which provide the values of y and $\dot{y}$ necessary for evaluating the right-hand sides of the energy equations. The $\dot{y}$'s enter the calculation via the voltages U_2 to U_4 according to (47), (48), and (49).

5. Determination of the magnetic circuit parameters

To calculate the currents and voltages according to the scheme shown in Fig. 6, we have to know the self-inductances L_j, the mutual inductances M_{jk} and the vertical field parameters ν, introduced by (63), of the various coils systems.

The basis for these calculations are the magnetic flux functions of the coils and the distribution of currents in the coils. The latter are the sources of the flux function fields, as is shown by (13).

To arrive at results which are reasonably simple, as are necessary for systems studies work of whole plants, we shall introduce some idealizations which will be presented in the next section.

5.1 Concept of the calculation

We start with the treatment of the following coils: transformer, vertical field, plasma chamber.

For an approximate calculation of the flux functions we use the procedure used in /4/. It mainly consists in idealizing a coil "a" as a toroidal shell with a circular minor cross-section (radius r_a) with infinitely thin wall (see Fig. 7). Within this wall the toroidal currents flow in the φ-direction. Because of the infinitely thin walls we have to treat the toroidal currents as surface currents $i_{\varphi a}$ which, in general, are functions of the poloidal angle ϑ. A current I_{a12} flowing across the sector between ϑ_1 and ϑ_2 in the φ-direction is thus given by

$$I_{a12} = r_a \int_{\vartheta_1}^{\vartheta_2} i_{\varphi a}(\vartheta)\, d\vartheta. \qquad (129)$$

We assume the surface current density $i_{\varphi a}(\vartheta)$ to be so smooth a function of ϑ that it may be represented by a Fourier series truncated after the third term:

$$i_{\varphi a}(\vartheta) = i_0 + i_1 \cos\vartheta + i_2 \cos 2\vartheta. \qquad (130)$$

This expansion contains only cosine terms because we assume symmetry of the coil currents with respect to z = 0 (corresponding to $\vartheta = 0$, and $\vartheta = \pi$ respectively).

The toroidal current carrying shell separates the two regions "1" and "2" from each other (see Fig. 7). Because in 1 and 2 no toroidal currents flow, the flux functions ψ_{a1} and ψ_{a2} pertaining to these regions have to obey (13) with $j_\varphi = 0$:

$$\frac{\partial^2 \psi_a}{\partial R^2} - \frac{1}{R}\frac{\partial \psi_a}{\partial R} + \frac{\partial^2 \psi_a}{\partial z^2} = 0. \qquad (131)$$

For the calculations to follow it is appropriate to transform equation (131) for ψ_a to the (r,ϑ) coordinate system. The result is

$$\frac{\partial^2 \psi_a}{\partial r^2} + \frac{1}{r}\frac{\partial \psi_a}{\partial r} + \frac{1}{r^2}\frac{\partial^2 \psi_a}{\partial \vartheta^2} - \frac{1}{R_a + r\cos\vartheta}\left(\cos\vartheta \frac{\partial \psi_a}{\partial r} - \frac{\sin\vartheta}{r}\cdot\frac{\partial \psi_a}{\partial \vartheta}\right) = 0. \qquad (132)$$

It follows from (9) that the r and ϑ components of B_{pol} are

$$B_r = -\frac{1}{2\pi R}\cdot\frac{1}{r}\cdot\frac{\partial \psi_a}{\partial \vartheta}, \qquad (133)$$

$$B_\vartheta = \frac{1}{2\pi R}\cdot\frac{\partial \psi_a}{\partial r} \qquad (134)$$

(here we have omitted the index "pol").

The existence of the surface current $i_{\varphi a}$ reflects in the fact that the poloidal magnetic induction $B_\vartheta(\vartheta)$ jumps according to

$$B_{\vartheta_1}(r_a, \vartheta) - B_{\vartheta_2}(r_a, \vartheta) = \mu_0\, i_{\varphi a}(\vartheta) \qquad (135)$$

if one goes from 1 to 2.

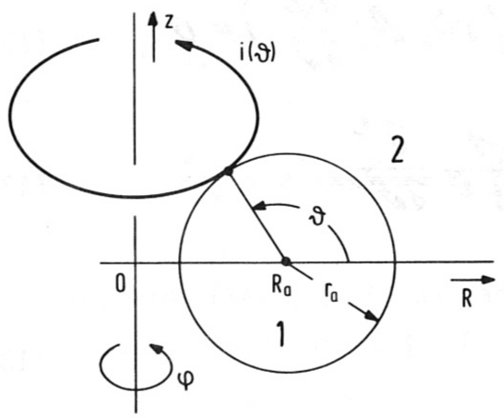

Fig. 7

This equation is a direct consequence of $\mathrm{rot}\vec{H} = \vec{j}$ and $\vec{B} = \mu_0\vec{H}$.

The next step of approximation is the most restrictive. It consists in assuming for each coil the ratio r_a/R_a of the minor radius and the major radius to be a small parameter of order ε. Furthermore, it is assumed that for any two coils "a" and "b" the ratio $(R_a - R_b)/r_a$ is also of order ε, which means that $(R_a - R_b)/R_a$ is of order ε^2.

In the case of the "plasma" we shall not assume surface currents but allow an arbitrary radial current distribution which does not depend on ϑ. Toroidicity is again allowed for to first order in ε.

The m a g n e t i c l i m i t e r coils shall be treated as strongly localized in space so that they are virtually toroidal current filaments.

The flux functions and current distributions together with $\psi = 2\pi RA\varphi$ and (34) yield the inductances $L_j = M_{jj}$ and M_{jk}.

The vertical field parameters ν_j are determined from the field $B_z(R_{pl}, z = 0)$ derived from the flux functions by using the defining equation (63).

5.2 Determination of the flux function for the thin shell approximation

We now return to the differential equation (132) for the flux function ψ_a. We introduce the normalized radial coordinate

$$\rho = r/r_a. \tag{136}$$

By treating $\varepsilon_a = r_a/R_a$ as small and truncating after first-order terms we get from (132)

$$\Delta\psi - \varepsilon_a \left(\cos\vartheta \cdot \frac{\partial\psi}{\partial\rho} - \frac{1}{\rho} \sin\vartheta \frac{\partial\psi}{\partial\vartheta} \right) = 0 \tag{137}$$

with

$$\Delta = \frac{\partial^2}{\partial\rho^2} + \frac{1}{\rho} \cdot \frac{\partial}{\partial\rho} + \frac{1}{\rho^2} \frac{\partial^2}{\partial\vartheta^2} \tag{138}$$

and

$$\varepsilon_a = r_a / R_a \tag{139}$$

(the index "a" of ψ has been omitted).

We now make the ansatz

$$\psi = \psi^{(0)} + \psi^{(1)} \tag{140}$$

with

$$\psi^{(1)}/\psi^{(0)} = O(\varepsilon_a).$$

If we introduce (140) into (137) and again restrict the result to zero and first-order terms, we get

$$\Delta\psi^{(0)} = 0 \,, \tag{141}$$

$$\Delta\psi^{(1)} = \varepsilon_a \left(\cos\vartheta \frac{\partial\psi^{(0)}}{\partial\rho} - \frac{1}{\rho}\sin\vartheta \frac{\partial\psi^{(0)}}{\partial\vartheta} \right). \tag{142}$$

Equation (142) can be solved by making the separation ansatz

$$\psi^{(0)} = \sum_{n=0}^{2} F_n(\rho) \cos n\vartheta \tag{143}$$

which already takes into account the mathematical form of our surface current distribution (130).

Substituting (143) in (141) yields

$$\psi_1^{(0)} = A_{01} + A_1 \rho \cos\vartheta + A_2 \rho^2 \cos 2\vartheta \,, \tag{144}$$

$$\psi_2^{(0)} = A_{01} + A_{02} \ln\rho + A_1 \rho^{-1} \cos\vartheta + A_2 \rho^{-2} \cos 2\vartheta . \tag{145}$$

The solution (144), (145) already takes into account the necessary nonsingular behaviour at $\rho = 0$ and $\rho \to \infty$ (except for the weak logarithmic singularity in (145)) and for continuity of ψ on the boundary $\rho = 1$. The latter is necessary because of div $\vec{B} = 0$. The logarithmic term in (145) can be tolerated because from the exact solution for the flux function of a ring carrying a uniform current it is known to be correct in the vicinity of $\rho = 1$. For $\rho \to \infty$ the exact flux function ψ vanishes. But this region obviously cannot be described by our small ε expansion.

The constant A_{01} will be determined by using formula (20) for the poloidal flux ϕ_{pol} and Maxwell's formula giving the e x t e r n a l inductance L of a ring with minor radius r_a carrying a uniform current:

$$L = \mu_0 R_a \left(\ln 8R_a/r_a - 2 \right). \tag{146}$$

From $\psi_2^{(0)} \to 0$ for $\rho \to \infty$, $\phi_{pol} = L(2\pi r_a i_o)$, L from (146), and formula (20) we get

$$A_{01} = 2\pi \mu_0 r_a R_a i_0 \left(\ln 8R_a/r_a - 2 \right). \tag{147}$$

The constant A_{02} follows from Ampère's law ($2\pi r B^{(0)} = -\mu_o 2\pi r_a i_o$) to be

$$A_{02} = -2\pi \mu_0 r_a R_a i_0 . \tag{148}$$

The constants A_1 and A_2 are determined from the surface condition

$$B_{\vartheta 1}^{(0)}(\rho=1,\vartheta) - B_{\vartheta 2}^{(0)}(\rho=1,\vartheta) = \mu_0 \left(i_0 + i_1 \cos\vartheta + i_2 \cos 2\vartheta \right). \tag{149}$$

The constant A_{02} already determined obviously also meets (149). The results for A_1 and A_2 are

$$A_1 = \frac{1}{2} \left(2\pi \mu_0 r_a R_a \right) i_1 , \tag{150}$$

$$A_2 = \frac{1}{4} \left(2\pi \mu_0 r_a R_a \right) i_2 . \tag{151}$$

Substituting the values of A_{01}, A_{02}, A_1, and A_2 (144) and (145) finally yields the zero-order flux functions $\psi_1^{(0)}$ and $\psi_2^{(0)}$:

$$\psi_1^{(0)}/2\pi\mu_0 r_a R_a = i_0 \left(\ln 8R_a/r_a - 2 \right) + \frac{1}{2} i_1 \rho \cos\vartheta + \frac{1}{4} i_2 \rho^2 \cos 2\vartheta , \tag{152}$$

$$\psi_2^{(0)}/2\pi\mu_0 r_a R_a = i_0 \left(\ln 8R_a/r_a\rho - 2 \right) + \frac{1}{2} i_1 \rho^{-1} \cos\vartheta + \frac{1}{4} i_2 \rho^{-2} \cos 2\vartheta . \tag{153}$$

Introducing the zero-order flux functions (152) and (153) into the differential equation (142) for the first-order flux function yields, respectively,

$$\Delta\psi_1^{(1)} = \varepsilon_a 2\pi\mu_0 r_a R_a \left(\frac{1}{2} i_1 + \frac{1}{2} i_2 \rho \cos\vartheta\right), \tag{154}$$

$$\Delta\psi_2^{(1)} = \varepsilon_a 2\pi\mu_0 r_a R_a \left(i_0 \rho^{-1} \cos\vartheta - \frac{1}{2} i_1 \rho^{-2} - \frac{1}{2} i_2 \rho^{-3} \cos\vartheta\right). \tag{155}$$

The solutions of (154) and (155) can be obtained analytically. The integration constants are determined from the continuity of $\psi^{(1)}$ at $\rho = 1$ and from the surface condition

$$B_{\vartheta 1}^{(1)}(\rho=1,\vartheta) - B_{\vartheta 2}^{(1)}(\rho=1,\vartheta) = 0 \tag{156}$$

to be met by the first-order contribution to B .

The latter condition is necessary because our surface current condition (130) is already taken into account by the zero-order equation (149). In this context it is important that the zero-order flux functions (152) and (153) produce first-order magnetic inductions because of the factor $1/R = 1/(R_a + r \cos\vartheta)$ in (134). The jump of this contribution to $B_\vartheta^{(1)}$ on $\rho = 1$ has to be cancelled by the B 's derived from $\psi^{(1)}$.

The results for $\psi_I^{(2)}$ and $\psi_2^{(1)}$ are

$$\psi_1^{(1)}/2\pi\mu_0 r_a R_a = \varepsilon_a \Big\{ C_1 + \frac{1}{8} i_1 (\rho^2 - 1) + \Big[C_2 + \frac{1}{16} i_2 (\rho^2 + 2) + \frac{1}{4} i_0\Big] \rho \cos\vartheta + \frac{3}{16} i_1 \rho^2 \cos 2\vartheta \Big\}, \tag{157}$$

$$\psi_2^{(1)}/2\pi\mu_0 r_a R_a = \varepsilon_a \Big\{ C_1 - \frac{1}{4} i_1 \ln\rho + \Big[C_2 \rho^2 - \frac{1}{2} i_0 \rho^2 \ln\rho + \frac{3}{16} i_2 + \frac{1}{4} i_0\Big] \rho^{-1} \cos\vartheta + \Big[\frac{1}{8} i_1 \rho^2 + \frac{1}{16} i_1\Big] \rho^{-2} \cos 2\vartheta \Big\}. \tag{158}$$

As was the case for the integration constant A_{01} in connection with the zero-order flux function, the constants C_1 and C_2 occurring in (157) and (158) can only be found by a comparison with an exact solution. They are given by

$$C_1 = \frac{1}{4} i_1 \left(\ln 8R_a/r_a - \frac{1}{2} \right) , \qquad (159)$$

$$C_2 = \frac{1}{2} i_0 \left(\ln 8R_a/r_a - 1 \right) . \qquad (160)$$

The total flux functions ψ_1 and ψ_2 are obtained by substituting $\psi_1^{(0)}$, $\psi_2^{(0)}$ (152, 153), $\psi_1^{(1)}$, $\psi_2^{(1)}$ (157, 158), and C_1, C_2 (159, 160) in (140). The result is

$$\begin{aligned} \psi_1/2\pi\mu_0 r_a R_a = \; & i_0 \left(\ln 8R_a/r_a - 2 \right) + \frac{1}{2} i_1 \rho \cos\vartheta + \frac{1}{4} i_2 \rho^2 \cos 2\vartheta \\ & + \varepsilon_a \Big\{ \frac{1}{4} i_1 \left(\ln 8R_a/r_a - \frac{1}{2} \right) + \frac{1}{8} i_1 (\rho^2 - 1) \\ & + \Big[\frac{1}{2} i_0 \left(\ln 8R_a/r_a - 1 \right) + \frac{1}{16} i_2 (\rho^2 + 2) \\ & + \frac{1}{4} i_0 \Big] \rho \cos\vartheta + \frac{3}{16} i_1 \rho^2 \cos 2\vartheta \Big\} , \end{aligned} \qquad (161)$$

$$\begin{aligned} \psi_2/2\pi\mu_0 r_a R_a = \; & i_0 \left(\ln 8R_a/r_a\rho - 2 \right) + \frac{1}{2} i_1 \rho^{-1} \cos\vartheta + \frac{1}{4} i_2 \rho^{-2} \cos 2\vartheta \\ & + \varepsilon_a \Big\{ \frac{1}{4} i_1 \left(\ln 8R_a/r_a\rho - \frac{1}{2} \right) + \Big[\frac{1}{2} i_0 \rho^2 \left(\ln 8R_a/r_a\rho - 1 \right) \\ & + \frac{3}{16} i_2 + \frac{1}{4} i_0 \Big] \rho^{-1} \cos\vartheta \\ & + \Big[\frac{1}{8} i_1 \rho^2 + \frac{1}{16} i_1 \Big] \rho^{-2} \cos 2\vartheta \Big\} . \end{aligned} \qquad (162)$$

The formulae (161) and (162) are identical with the results given in /4/ (eqs. 11' and 12'), as can be seen after some ordering and the introduction of ε_a and our normalized coordinate ρ instead of the ρ used in /4/.

5.3 Flux function of the plasma

The determination of the plasma flux function ψ_{pl} has to take into account a toroidal current density distribution. Furthermore, the pressure balance

$$\vec{j} \times \vec{B} = \mathrm{grad}\, p \tag{163}$$

has to be met. For a circular minor plasma cross-section with radius r_{pl} the result up to first-order terms in ε is given in /3/. Transcription to our nomenclature and coordinate system leads to the flux function outside the plasma:

$$\psi_{pl} / \mu_0 R_{pl} I_{pl} = \left(\ln \frac{8 R_{pl}}{r_{pl}\, \rho} - 2 \right) + \varepsilon_{pl} \frac{1}{2} \left[\rho^2 \left(\ln \frac{8 R_{pl}}{r_{pl}\, \rho} - 1 \right) + \left(\lambda_1 + \frac{1}{2} \right) \right] \rho^{-1} \cos \vartheta . \tag{164}$$

The parameter λ_1 is given by (61); $\varepsilon_{pl} = r_{pl}/R_{pl}$ is the analogon to ε_a. The current distribution is assumed to be independent of ϑ.

5.4 Self-inductances

In the following we shall calculate the self-inductances of the plasma ring, transformer primary winding, vertical field coils, magnetic limiter coils, and plasma chamber.

5.4.1 Self-inductance of the plasma ring

The self-inductance L_1 of the plasma ring is given by the sum of the internal and external inductances:

$$L_1 = L_{1i} + L_{1e} . \tag{165}$$

From (62) we get

$$L_{1i} = L_{pl,i} = \mu_0 R_{pl}\, l_i/2 . \tag{166}$$

From (34) and (6) we get

$$L_{1e} = M_{me} = \frac{1}{I_{pl}^2}\int_0^{2\pi}\int_0^{2\pi} \frac{\psi_{pl}(\rho=1,\vartheta)}{2\pi R_{pl}}\, i_0\, r_{pl} R_{pl}\, d\vartheta\, d\varphi . \tag{167}$$

Substituting ψ_{pl} from (164) in (166) yields upon integration

$$L_{1e} = \mu_0 R_{pl}\left(\ln {}^{8R_{pl}}/_{r_{pl}} - 2\right) . \tag{168}$$

Equation (165) together with (166) and (168) gives

$$L_1 = \mu_0 R_{pl}\left(\ln {}^{8R_{pl}}/_{r_{pl}} - 2 + l_i/2\right) . \tag{169}$$

5.4.2 Self-inductance of the transformer primary winding

To minimize the disturbance of the plasma by the field of the primary winding, we impose the condition

$$\vec{B}_{tr} \equiv 0 \quad , \quad \rho < 1 \tag{170}$$

which means $\psi_{1,tr}$ = const for $\rho < 1$. Up to order $\varepsilon_{tr} = r_{tr}/R_{tr}$ this can be achieved by

$$i_{tr} = i_0 - \varepsilon_{tr}\, i_0 \left(\ln {}^{8R_{tr}}/_{r_{tr}} - \frac{1}{2}\right)\cos\vartheta . \tag{171}$$

Equation (171) follows from the condition that the terms containing ρ, $\cos\vartheta$, and $\cos 2\vartheta$ in (161) have to vanish. The surface current density i_0 is related to the transformer current I_2 and to the number of turns N_{tr} by

$$\int_0^{2\pi} i_{tr}\, r_{tr}\, d\vartheta = N_{tr} I_{tr} = N_{tr} I_2 . \tag{172}$$

Equation (172) expresses the condition that the ampere turns of the real transformer coil have to be identical with those of our continuous model. The result for i_0 is

$$i_0 = N_{tr} I_{tr} / 2\pi r_{tr} . \tag{173}$$

The corresponding flux function inside the transformer coil is given by

$$\psi_{1,tr} = \mu_0 R_{tr} N_{tr} I_{tr} \left(\ln 8R_{tr}/r_{tr} - 2 \right) . \tag{174}$$

By analogy with (167) the transformer inductance L_2 is given by

$$L_2 = M_{22} = \frac{1}{I_{tr}^2} \int_0^{2\pi} \psi_{1,tr}(\rho = 1, \vartheta)\, i_{tr}\, r_{tr}\, d\vartheta \tag{175}$$

where the integration over φ has already been performed. By inserting $\psi_{1,tr}$ from (174) and i_{tr} from (171), (173) we get from (175)

$$L_2 = \mu_0 R_{tr} N_{tr}^2 \left(\ln 8R_{tr}/r_{tr} - 2 \right) . \tag{176}$$

5.4.3 Self-inductance of the vertical field coil system

In accordance with /4/ we use the following surface current distribution in the vertical field coil system:

$$i_v = i_{v1} \cos\vartheta + \alpha i_{v1} \cos 2\vartheta . \tag{177}$$

This current distribution leads to a dipole magnetic field with a quadrupole correction if $\alpha \neq 0$. The latter is necessary because axial and radial stability of the plasma equilibrium position is only assured if the decay index n_v of the vertical field

$$n_v = - \frac{R_{pl}}{B_v} \cdot \frac{\partial B_v}{\partial R} \bigg|_{R=R_{pl}} \tag{178}$$

meets the condition /3, p. 610/

$$0 < n_v < 3/2 . \tag{179}$$

The value of n_v can be adjusted by varying α.

The current distribution (177) is shown schematically in Fig. 8. The current flows within the two regions $-\vartheta_v \le \vartheta \le \vartheta_v$ and $\vartheta_v \le \vartheta \le (2\pi - \vartheta_v)$. The net toroidal current in the vertical field coils is zero. We define the vertical field current $I_v = I_3$ by

$$N_v I_v = r_v \int_{-\vartheta_v}^{\vartheta_v} i_v \, d\vartheta . \tag{180}$$

N_v is the number of turns belonging to one of the two regions of current flow mentioned above.

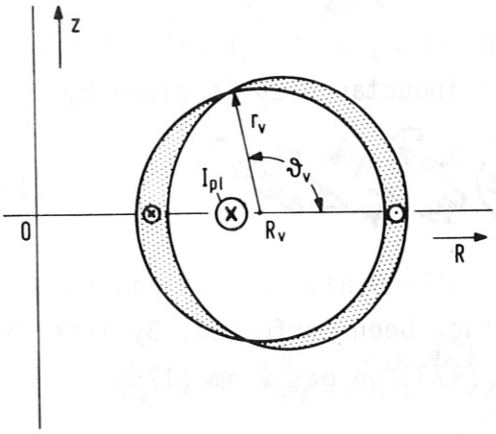

Fig. 8

By inserting i_v from (177) into (180) we get upon integration

$$i_{v1} = N_v I_v / 2k r_v \tag{181}$$

with

$$k = \left(\frac{4\alpha^2 - 1 + \sqrt{1+8\alpha^2}}{8\alpha^2} \right)^{1/2} \left(1 + \frac{\sqrt{1+8\alpha^2} - 1}{4} \right) . \tag{182}$$

By means of (181) we can rewrite i_v from (177) in the following form:

$$i_v = \frac{1}{2k r_v} N_v I_v \left(\cos\vartheta + \alpha \cos 2\vartheta \right) . \tag{183}$$

The corresponding flux function $\psi_{1,v}$ follows upon replacing in (161) i_o by 0 and i_1, i_2 by the corresponding currents read from (183). The result is

$$\psi_{1,v} = \mu_0 \frac{\pi}{16k} R_v N_v I_v \Big\{ 8\rho\cos\vartheta + 4\alpha\rho^2 \cos 2\vartheta + \varepsilon_v \Big[4\Big(\ln \frac{8R_v}{r_v} - \frac{1}{2}\Big) + 2(\rho^2 - 1) + 3\rho^2 \cos 2\vartheta \Big] \Big\} \tag{184}$$

with $\varepsilon_v = r_v/R_v$. In the derivation of (184) we have already used the fact that α is of order ε_v, as will be demonstrated in the following.

The vertical field produced by the flux function $\psi_{1,v}$ in the symmetry plane $z = 0$ is given by

$$B_v(R) = \frac{1}{2\pi R} \cdot \frac{\partial \psi_{1,v}}{\partial R}\Big|_{z=0} = \frac{1}{2\pi R} \cdot \frac{\partial \psi_{1,v}}{\partial \rho}\Big|_{\substack{\vartheta=0 \\ \vartheta=\pi}} \cdot \frac{1}{\varepsilon_v R_v} \, . \tag{185}$$

Whether we have to use $\vartheta = 0$ or $\vartheta = \pi$ in (185) depends on R being greater or smaller than R_v.

Inserting $\psi_{1,v}$ from (184) into (185) yields

$$B_v(R) = \frac{\mu_0}{16k} \frac{N_v I_v}{r_v} \Big[4 + \Big(4\frac{\alpha}{\varepsilon_v} + 1\Big) \frac{R - R_v}{R_v} \Big] . \tag{186}$$

From (186) we can calculate n_v as a function of R_{pl} using (178). The result is

$$n_v = - \frac{(4\alpha + \varepsilon_v) R_{pl}}{4\varepsilon_v R_v + 4\alpha(R_{pl} - R_v) + 9\varepsilon_v (R_{pl} - R_v)} \, . \tag{187}$$

If some stability criterion such as (179) is used to prescribe the value of n_v, the corresponding value of α is found from (187) to be

$$\alpha = - \frac{\varepsilon_v}{4} \cdot \frac{R_{pl} + 4n_v R_{pl} + 5n_v(R_{pl} - R_v)}{R_{pl} + n_v(R_{pl} - R_v)} \, . \tag{188}$$

Because of our assumption $(R_{pl} - R_v)/R_v = O(\varepsilon^2)$ equation (188) reduces in first order to

$$\alpha = -\varepsilon_v (l_v + 1/4). \tag{189}$$

Equation (188) shows that α is of order ε_v, as already used in deriving the flux function (184). Equation (189) coincides with the result for $R_{pl} = R_v$ given in /4, p. 13/, whereas the general formula (188) does not.

From

$$L_3 = \frac{1}{I_v^2} \int_0^{2\pi} \Psi_{1,v}(\rho = 1, \vartheta)\, i_v\, r_v\, d\vartheta \tag{190}$$

we get with i_v from (177) and by restriction to terms up to order ε_v

$$L_3 = \mu_0 \frac{\pi^2}{4k^2} R_v N_v^2 \tag{191}$$

This formula coincides with the result given in /4, p. 21/.

5.4.4 Self-inductances of the plasma chamber components

We assume the following surface current distribution in the chamber wall:

$$i_c = i_{c0} + i_{c1} \cos\vartheta + i_{c2} \cos 2\vartheta. \tag{192}$$

Equation (192) is a Fourier expansion of the surface current distribution induced in the chamber wall, truncated after the third term. This distribution is shown schematically in Fig. 9. The terms in (192)

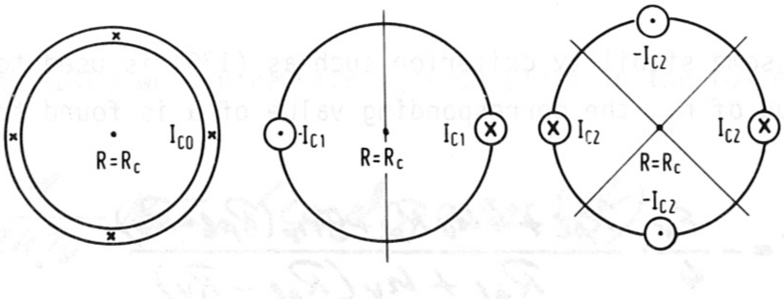

Fig. 9

correspond to the mean toroidal chamber current and to dipole and quadrupole toroidal current distributions. The mean current can be suppressed by a poloidal slit in the chamber wall.

The three chamber currents I_{C0}, I_{C1}, and I_{C2} are defined by

$$I_{C0} = r_c \int_0^{2\pi} i_{C0}\, d\vartheta , \tag{193}$$

$$I_{C1} = r_c \int_{-\pi/2}^{\pi/2} i_{C1} \cos\vartheta \cdot d\vartheta \tag{194}$$

$$I_{C2} = r_c \int_{-\pi/4}^{\pi/4} i_{C2} \cos 2\vartheta \cdot d\vartheta . \tag{195}$$

From (193) to (195) we get the i_{C0}, i_{C1}, and i_{C2}, which when inserted in (192) yield

$$i_c = I_{C0}/2\pi r_c + I_{C1}/2r_c \cdot \cos\vartheta + I_{C2}/r_c \cdot \cos 2\vartheta . \tag{196}$$

By introducing i_{C0}, i_{C1}, and i_{C2} into the flux function (161) we get for the chamber flux function $\psi_{1,C}$:

$$\psi_{1,C} = \psi_{1,C0} + \psi_{1,C1} + \psi_{1,C2} , \tag{197}$$

$$\psi_{1,C0} = \mu_0 R_c I_{C0} \Big[(\ln 8R_c/r_c - 2) + \varepsilon_c \Big[\tfrac{1}{2} (\ln 8R_c/r_c - 1) + \tfrac{1}{4} \Big] \rho \cos\vartheta \Big] , \tag{198}$$

$$\psi_{1,C1} = \mu_0 \pi R_c I_{C1} \Big[\tfrac{1}{2} \rho \cos\vartheta + \varepsilon_c \Big[\tfrac{1}{4} (\ln 8R_c/r_c - \tfrac{1}{2}) + \tfrac{1}{8} (\rho^2 - 1) + \tfrac{3}{16} \rho^2 \cos 2\vartheta \Big] \Big] , \tag{199}$$

$$\psi_{1,C2} = \mu_0 2\pi R_c I_{C2} \Big[\tfrac{1}{4} \rho^2 \cos 2\vartheta + \varepsilon_c \tfrac{1}{16} \rho (\rho^2 + 2) \cos\vartheta \Big] . \tag{200}$$

The three self-inductances L_5, L_6, and L_7 corresponding to the three chamber current components I_{C0}, I_{C1}, and I_{C2} are given by

$$L_5 = \frac{r_c}{I_{C0}^2} \int_0^{2\pi} \psi_{1,C0} (\rho = 1, \vartheta)\, i_{C0}\, d\vartheta , \tag{201}$$

$$L_6 = \frac{r_c}{I_{C1}^2}\int_0^{2\pi}\psi_{1,C1}(\rho=1,\vartheta)\,i_{C1}\cos\vartheta\,d\vartheta, \tag{202}$$

$$L_7 = \frac{r_c}{I_{C2}^2}\int_0^{2\pi}\psi_{1,C2}(\rho=1,\vartheta)\,i_{C2}\cos 2\vartheta\,d\vartheta. \tag{203}$$

With i_{C0}, i_{C1}, and i_{C2} read from (196) we get from (201) to (203)

$$L_5 = \mu_0 R_c\left(\ln 8R_c/r_c - 2\right), \tag{204}$$

$$L_6 = \mu_0 \frac{\pi^2}{4} R_c, \tag{205}$$

$$L_7 = \mu_0 \frac{\pi^2}{2} R_c. \tag{206}$$

These formulae coincide with the results given in /4, p. 20/.

5.4.5 Self-inductance of a magnetic limiter coil system.

It is assumed that one magnetic limiter coil system consists of a triple of current carrying rings such as is schematically shown in Fig. 10. The sum of the ampere turns of the two excentric coils is equal to the ampere turns of the central coil but opposite in sign. We assume that the current in each turn is the same for all coils and is the current $I_4 = I_{ml}$, which occurs in the circuit equations (46) to (52).

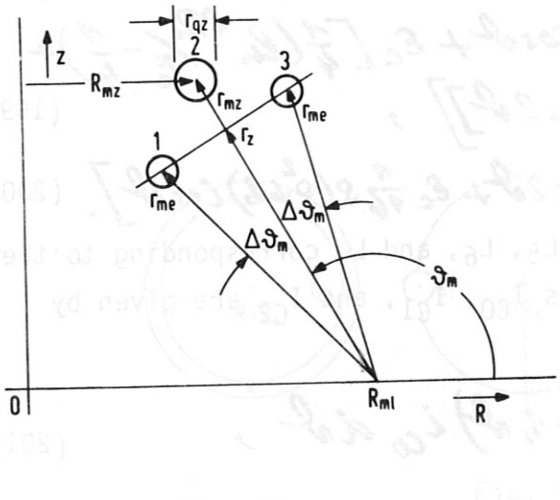

Fig. 10

The net current in one triple is zero. In actual tokamak devices there may exist two triples arranged symmetrically with respect to z = 0 (i.e. ASDEX, PDX) or one triple at, for instance, $\vartheta = 0$ (i.e. JT-60).

Within our accuracy requirements the inductance of a ring carrying a uniform current is given by the well-known formula

$$L = \mu_0 R_i \left(\ln 8R_i/r_q - 7/4 \right). \qquad (207)$$

R_i is the major ring radius, r_q is the radius of the minor cross--section, which is assumed to be circular. Equation (207) emerges from a formula already given by Maxwell for $r_q/R \ll 1$. By the way, eq. (207) is the same formula as the plasma inductance (169) for $l_i = 0.5$, which is the normalized internal inductance of a uniform toroidal current distribution.

If the minor cross-section is not circular, an equivalent minor radius can be calculated from the cross-sectional area A_q by

$$r_{eq} = (A_q/\pi)^{1/2}. \qquad (208)$$

This radius r_{eq} introduced in (207) gives results for L which are completely sufficient within our accuracy requirements. This can be seen from, for example, the formula valid for a rectangular minor cross-section with cross-sectional lengths a and b /5, p. 13/:

$$L = \mu_0 R_i \left(\ln \frac{8R_i}{a+b} - 0{,}501 \right). \qquad (209)$$

For a square cross-section (a = b) the formulae (208) and (209) lead to

$$L = \mu_0 R_i \left(\ln 8R_i/r_{eq} - 1.7665 \right) \qquad (210)$$

which is sufficiently close to (207).

The mutual inductance M of two rings with major radii R_i and R_j can be calculated with sufficient accuracy by indealizing the rings to circular current filaments located at the centres of the two rings. The result for M is /6, p. 364)

$$M = \mu_0 (R_i R_j)^{1/2} \left[\left(\frac{2}{k} - k\right) F(\pi/2, k) - \frac{2}{k} E(\pi/2, k) \right] \tag{211}$$

with

$$k^2 = \frac{4 R_i R_j}{\Delta z_{ij}^2 + (R_i + R_j)^2} = 1 - k_1^2 = 1 - \left(\frac{d_{ij}}{e_{ij}}\right)^2 , \tag{212}$$

$$F(\alpha, k) = \int_0^{\alpha} (1 - k^2 \sin^2 \alpha')^{-1/2} \, d\alpha' , \tag{213}$$

$$E(\alpha, k) = \int_0^{\alpha} (1 - k^2 \sin^2 \alpha')^{1/2} \, d\alpha' . \tag{214}$$

E and F are the (incomplete) elliptical integrals of the first and second kinds. The geometrical arrangement is shown in Fig. 11.

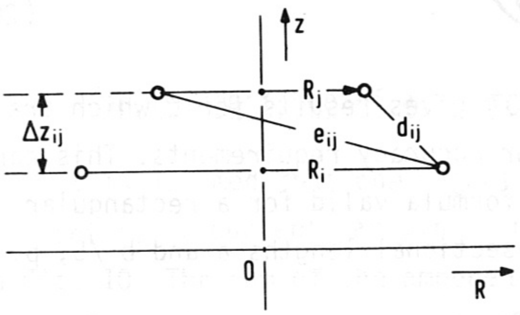

Fig. 11

A series expansion of the elliptical integrals occurring in (211) leads to the following formula for M, which is especially suitable for coaxial rings placed closely together (5, p.6):

$$M = \mu_0 (R_i R_j)^{1/2} \left(\ln \frac{e_{ij}}{d_{ij}} - 0{,}6137 \right). \tag{215}$$

The self-inducatance L_{ml} of one magnetic limiter coil triple is given by the double sum over all coupling inductances between the three coils:

$$L_{ml} = \sum_{j=1}^{3} \sum_{i=1}^{3} M_{ij} . \tag{216}$$

With

$$L_i = M_{ii}$$

and because of $M_{ij} = M_{ji}$ we get from (216)

$$L_{ml} = L_1 + L_2 + L_3 + 2(M_{12} + M_{23} + M_{13}). \qquad (217)$$

The self-inductances L_1, L_2, L_3 and the mutual inductances M_{12}, M_{23}, M_{13} follow from (210) and (216) respectively by multiplication by the appropriate number of turns and by introducing the appropriate geometrical data (R_i, R_j, r_q, d_{ij}, e_{ij}). The numbers of turns are given by

$$N_1 = -1/2 \cdot N_{mz} ,$$

$$N_2 = N_{mz} ,$$

$$N_3 = -1/2 \cdot N_{mz} .$$

N_{mz} is the number of turns of the central coil of the triple.

The distances between the three limiter coils projected onto a plane φ= const (i.e. the plane shown by Fig. 10) normalized to the major radius R_{ml} are of the order

$$\Delta\varepsilon = \varepsilon_{mz} - \varepsilon_{ml} \qquad (218)$$

with

$$\varepsilon_{mz} = r_{mz} / R_{ml} , \qquad (219)$$

$$\varepsilon_{ml} = r_{ml} / R_{ml} . \qquad (220)$$

Obviously, $\Delta\varepsilon$ is of the order of the angle $\Delta\vartheta_m$ (see Fig. 10). In the evaluation of (207) and (215) we treat $\Delta\vartheta_m$ as a small parameter which is only taken into account up to first order. In contrast to the preceding calculation we shall not treat ε_{mz} and ε_{me} as small parameters because this would not lead to a significant simplification of the calculations.

After lengthy computation the magnetic limiter self-inductance $L_4 = L_{ml}$ is found to be

$$L_4 = \mu_0 R_{ml} N_{mz}^2 \Big[(1+\varepsilon_{mz} \cos\vartheta_m) \times \ln \frac{8R_{ml}(1+\varepsilon_{mz}\cos\vartheta_m)\left[(\varepsilon_{mz}-\varepsilon_{me})^2+\varepsilon_{mz}\varepsilon_{me}(\Delta\vartheta_m)^2\right]}{r_{qz}\left[2+(\varepsilon_{mz}+\varepsilon_{me})\cos\vartheta_m\right]^2} + \frac{1}{2}(1+\varepsilon_{me}\cos\vartheta_m)\ln\frac{8R_{ml}(1+\varepsilon_{me}\cos\vartheta_m)^2}{r_{qz}\,\varepsilon_{me}\,\Delta\vartheta_m} + (0{,}2274\,\varepsilon_{mz}+0{,}6932\,\varepsilon_{me})\cos\vartheta_m - 1{,}5312 \Big]. \quad (221)$$

5.5 Mutual inductances between components with currents distributed over volume or surface

In this section we calculate the mutual inductances between all coils except the magnetic limiter coil system. All the remaining coil systems are characterized by the fact that the interacting magnetic fields are produced by currents flowing in the volume or on the surface of the components considered.

A current I_j flowing in a component produces a flux function $\psi_j(\rho,\vartheta)$. According to the truncated Fourier expansion which we have used for the current densities the general form of ψ_j is given by

$$\psi_j / 2\pi\mu_0 R_j = I_j \left[F_0(\rho)+F_1(\rho)\cos\vartheta+F_2(\rho)\cos 2\vartheta\right]. \quad (222)$$

Examples are the flux function (164) of the plasma and those for the thin-shell approximation (161, 162). In the latter one has to insert the relations between the surface currents i_j and the total currents I_j, which are given in Sections 5.4.2 to 5.4.4. The flux function ψ_j interacts with a surface current distribution i_k, which we write in the general form

$$i_k(\vartheta) = I_k(f_0 + f_1\cos\vartheta + f_2\cos 2\vartheta). \quad (223)$$

The constants f_o, f_1, and f_2 for an actual distribution $i_k(\vartheta)$ can be read from the distributions $i_{tr}(\vartheta)$, $i_v(\vartheta)$, and $i_c(\vartheta)$ given in Sections 5.4.2 to 5.4.4.

The geometrical arrangement of the component j producing ψ_j and the component k which carries the current density i_k is shown in Fig. 12.

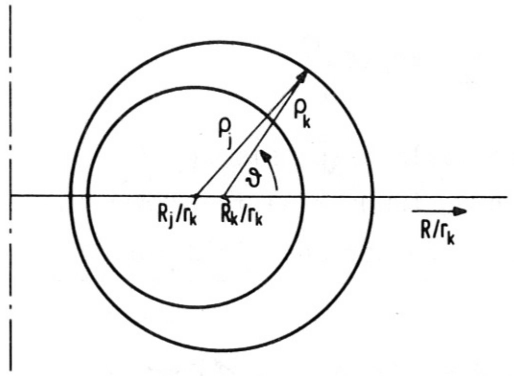

Fig. 12

Because the currents i_k flow across the circle $r = r_k$ (as shown in Fig. 7 for $i(\vartheta)$ with $r_k = r_a$) it is convenient to normalize the radii r to r_k. The current thus flows across the circle $\rho_k = 1$. To be consistent with this normalization, we have to replace the coordinate ρ occurring in the flux functions of Sections 5.3 and 5.4.2 to 5.4.4 according to

$$\rho = \rho_j \frac{r_k}{r_j} \quad . \qquad (224)$$

The relation between the normalized coordinates ρ_j and ρ_k is given by

$$\rho_j^2 = \rho_k^2 + (R_k - R_j)^2/r_k^2 + 2\rho_k (R_k - R_j)/r_k \cdot \cos\vartheta \, . \qquad (225)$$

As already mentioned, we shall assume in the following that

$$\Delta = (R_k - R_j)/r_k$$

is of order ε . Up to first order in ε we get from (225)

$$\rho_j = \rho_k + \Delta \cos\vartheta \qquad (226)$$

To the same order we approximate the flux function $\psi_j(\rho = \rho_j r_k/r_j)$ by the truncated Taylor expansion

$$\psi_j\left(\rho = \rho_j \frac{r_k}{r_j}\right) = \psi_j\left(\rho = \rho_k \frac{r_k}{r_j}\right) + \frac{\partial \psi_j}{\partial \rho}\left(\rho = \rho_k \frac{r_k}{r_j}\right) \Delta \cos\vartheta \qquad (227)$$

The mutual inductance M_{jk} follows from (34) and (6) to be

$$M_{jk} = \frac{1}{I_j I_k} \int_0^{2\pi} \psi_j \left(\rho_j \frac{r_k}{r_j}, \vartheta \right) i_k(\vartheta) \, d\vartheta \tag{228}$$

where we have replaced $j_\varphi dV$ by $i_k \, 2\pi r_k \, d\vartheta$.

We now insert ψ_j from (222) in the Taylor expansion (227) and introduce the result together with i_k from (223) in (228). The resulting integrals can easily be performed and yield for M_{jk}

$$M_{jk}/2\pi^2\mu_0 R_j r_k = 2f_0F_0 + f_1F_1 + f_2F_2 + \Delta\left(f_0F_{1\rho} + f_1F_{0\rho} + \tfrac{1}{2}f_1F_{2\rho} + \tfrac{1}{2}f_2F_{1\rho}\right) \tag{229}$$

with

$$F_n = F_n\left(\rho = \rho_k \frac{r_k}{r_j}\right), \tag{230}$$

$$F_{n\rho} = \frac{dF_n}{d\rho}\left(\rho = \rho_k \frac{r_k}{r_j}\right), \quad n = 1, 2, 3. \tag{231}$$

Formula (230) shows that the displacement $R_k - R_j = \Delta . r_k$ of the two coil centres contributes to the mutual inductance.

5.5.1 Plasma-transformer inductance

The F_n and $F_{n\rho}$ are calculated by using the plasma flux function (164), while the f_n are yielded by the transformer current distribution (171). Insertion of these values in (229) yields

$$M_{12} = M_{pl,tr} = \mu_0 R_{tr} N_{tr} \left(\ln 8R_{tr}/r_{tr} - 2 \right). \tag{232}$$

if terms of second order in ε are neglected. In this connection it is important that all major radii R differ from each other only to second order because Δ is treated as a first order term in ε.

5.5.2 Plasma-vertical field inductance

The F_n and $F_{n\varsigma}$ are calculated by using the plasma flux function (164), while the f_n are yielded by the vertical field current distribution (183). By accounting for the fact that α is of the order ε_v we get the result

$$M_{13} = M_{pl,v} = \frac{1}{4k}\mu_0 \pi R_v N_v \Big[\varepsilon_v\left(\ln 8R_v/r_v - 1\right) + \varepsilon_{pl}\left(r_{pl}/r_v\right)\left(\lambda_1 + 1/2\right) + 2/r_v \cdot \left(R_{pl} - R_v\right)\Big]. \qquad (233)$$

Because $\mu_0 R_k N_j N_k$ gives the zeroth order of a mutual inductance M_{jk} one can see from (233) that $M_{pl,v}$ is only a first-order quantity. This means that the magnetic interaction energy between plasma and vertical field is due to toroidal curvature, to the relative displacement of the coil centers, and to the dipole character of the vertical field.

5.5.3 Plasma-chamber inductances

The calculation of the mutual inductances between the plasma and the chamber current components I_{c0}, I_{c1}, and I_{c2} is again based on the plasma flux function (164).

For calculating $M_{15} = M_{pl,c}$, one has to identify i_k from (233) with the first term $(I_{c1}/2\pi r_c)$ of the chamber current distribution (196). We thus get $f_o = 1/2\pi r_c, f_1 = f_2 = 0$. The result for M_{15} is

$$M_{15} = M_{pl,c0} = \mu_0 R_c \left(\ln 8R_c/r_c - 2\right). \qquad (234)$$

The analogous procedure for the current components I_{C1} and II_{C2} leads to

$$M_{16} = M_{pl,c1} = \frac{1}{4}\mu_0 \pi R_c \Big[\varepsilon_c\left(\ln 8R_c/r_c - 1\right) + \varepsilon_{pl}\left(r_{pl}/r_c\right)\left(\lambda_1 + 1/2\right) + 2/r_c \left(R_{pl} - R_c\right)\Big], \qquad (235)$$

$$M_{17} = M_{pl,c2} = 0. \qquad (236)$$

$M_{pl,c1}$ is a first-order quantity, while $M_{pl,c2}$ is zero in first order.

5.5.4 Transformer-vertical field inductance

For ease of calculation we identify ψ_j in (228) with the flux function $\psi_{1,tr}$ (174), which is valid inside the transformer coils. The vertical field current distribution $i_v(\vartheta)$ according to (183) contains only terms proportional to $\cos\vartheta$ and $\cos 2\vartheta$. This leads to M = 0 - as can immediately be seen from the integral (228) - because $\psi_{1,tr}$= const:

$$M_{23} = M_{tr,v} = 0. \tag{237}$$

5.5.5 Transformer-chamber inductances

The calculation is again based on the constant flux function $\psi_{1,tr}$. Because of this constancy the integral (228) can be directly evaluated by inserting the three components of $i_c(\vartheta)$ according to (196). The resulting mutual inductances are

$$M_{25} = M_{tr,co} = \mu_0 R_{tr} N_{tr} \left(\ln {}^{8R_{tr}}/_{r_{tr}} - 2\right), \tag{238}$$

$$M_{26} = M_{tr,c1} = 0, \tag{239}$$

$$M_{27} = M_{tr,c2} = 0. \tag{240}$$

The mutual inductance $M_{tr,co}$ is a zero-order quantity.

5.5.6 Vertical field-chamber inductances

The F_n and $F_{n\rho}$ are calculated from the flux function $\psi_{1,v}$ which is valid inside the vertical field coils. The components of the chamber current distribution are read from $i_c(\vartheta)$ according to (196) and yield the f_n. The mutual inductances resulting from (229) are

$$M_{35} = M_{v,co} = \frac{1}{4\pi}\mu_0 \pi R_v N_v \Big[E_v\left(\ln {}^{8R_v}/_{r_v} - 1\right) + \frac{1}{2} E_v \left({}^{r_c}/_{r_v}\right)^2 - \left({}^{1}/_{r_v}\right)\cdot\left(R_v - R_c\right)\Big], \tag{241}$$

$$M_{36} = M_{V,C1} = \frac{1}{4k} \mu_0 \tilde{r}^2 R_V N_V (r_c/r_V) , \tag{242}$$

$$M_{37} = M_{V,C2} = \frac{1}{4k} \mu_0 \tilde{r}^2 R_V N_V (r_c/r_V)^2 \times \left[\frac{3}{4}\varepsilon_V + \alpha - (r_V/r_c^2)(R_V - R_c)\right]. \tag{243}$$

The mutual inductance $M_{V,C1}$ is of zeroth order. The remaining inductances $M_{V,C0}$ and $M_{V,C2}$ are of order ε and are due to coupling by toroidal curvature and relative displacement.

5.5.7 Mutual inductances of the plasma chamber current components

These mutual inductances can again be calculated directly from the integral (228). By inserting $\psi_{1,c0}$ according to (198) and the second term of $i_c(\vartheta)$ from (196) we get

$$M_{56} = M_{C0,C1} = \frac{1}{4} \mu_0 \tilde{r} R_c \varepsilon_c \left(\ln 8R_c/r_c - \frac{1}{2}\right). \tag{244}$$

In an analogous way we get $M_{c0,c2}$ from $\psi_{1,c0}$ and the third term of $i_c(\vartheta)$ as well as $M_{c1,c2}$ from $\psi_{1,c1}$ according to (199) together with the same component of $i_c(\vartheta)$:

$$M_{57} = M_{C0,C2} = 0 , \tag{245}$$

$$M_{67} = M_{C1,C2} = \frac{3}{16} \mu_0 \tilde{r}^2 R_c \varepsilon_c . \tag{246}$$

Again, as in previous cases, the coupling is due to toroidal curvature and is thus of order ε at the most.

5.5.8 Compilation of the orders of the inductances

For systems studies work computing time may play an important role. We therefore represent the order of the various inductances in matrix form to facilitate a quick assessment of useful accuracy. In most cases the first-order inductances are given sufficiently accurately by the procedure used. Zero-order inductances may in some cases call for higher precision and then have to be calculated by a better analysis or by a computer code based on the evaluation of elliptic integrals. If the order of an inductance is at the most of order ε^2 it is marked by 0 in Table 1. The results involving component "4" (magnetic limiter coils) are collected from Sections 5.6.1 to 5.6.4.

component	1	2	3	4	5	6	7
1	1						
2	1	1					
3	ε	0	1				
4	ε	0	ε	1			
5	1	1	ε	ε	1		
6	ε	0	1	ε	ε	1	
7	0	0	ε	ε	0	ε	1

Table 1

In passing we note that all inductances for distributed currents coincide with those given in /4/ except for two cases. These are M_{35} and M_{37}: The last term of M_{35} in our case is a factor of 2 larger than in /4/. In M_{37} we get a term proportional to $(R_V - R_C)$, which is missing in /4/.

5.6 Mutual inductances between one set of magnetic limiter coils and the components with distributed currents

The geometrical arrangement of one magnetic limiter coil triple already been shown in Fig. 10. For calculating the mutual inductances between the limiter coils and the other components we neglect the radial extents of the limiter coil cross-sections by treating them as line currents. The corresponding distribution of the current density j_{ml} is given by

$$j_{ml}(r,\vartheta) = I_{ml} N_{mz} \Big[\frac{1}{r_{mz}} \delta(r_k - r_{mz}) \delta(\vartheta_k - \vartheta_m) - \frac{1}{2 r_{me}} \delta(r_k - r_{me}) \delta(\vartheta_k - \vartheta_m + \Delta\vartheta_m) - \frac{1}{2 r_{me}} \delta(r_k - r_{me}) \delta(\vartheta_k - \vartheta_m - \Delta\vartheta_m) \Big] \qquad (247)$$

(r_k and ϑ_k are the coordinates with respect to $R = R_{ml}$, $z = 0$, as shown in Fig. 13).

From (34) and (6) we get for the mutual inductance $M_{j,ml}$ between a coil system j and the magnetic limiter triple

$$M_{j,ml} = \frac{1}{I_j I_{ml}} \int_V \frac{1}{2\pi R} \psi_j \, j_{ml} \, dV . \tag{248}$$

ψ_j is the flux function produced by the current I_j flowing in the coil system j. By inserting j_{ml} from (247) in (248) and using

$$dV = 2\pi R \, dr_k \cdot r_k \, d\vartheta_k \tag{249}$$

we get for $M_{j,ml}$

$$M_{j,ml} = \frac{N_{mz}}{I_j} \Big[\psi_j(r_{mz}, \vartheta_m) - \frac{1}{2}\psi_j(r_{ml}, \vartheta_m - \Delta\vartheta_m) - \frac{1}{2}\psi_j(r_{ml}, \vartheta_m + \Delta\vartheta_m) \Big] . \tag{250}$$

Formula (250) can also be found by using the fact that $M_{j,ml}$ describes the amount of flux produced by the coil j and interlinked with the triple coils and using the relation (20) between the magnetic flux ϕ_{pol} and the flux function ψ_j.

The flux functions ψ_j. which we have given in Sections 5.3 and 5.4.1 to 5.4.4, are centred at $R = R_j$, $z = 0$, which may be shifted with respect to $R = R_{ml}$, $z = 0$. This leads to the differences between r_k, ϑ_k and r, ϑ shown in Fig. 13.

We again treat $\Delta R/r_k = (R_{ml}-R_j)r_k$ as a quantity or order ε. By analogy with (226) this leads to

$$r = r_k + \Delta R \cos\vartheta_k . \tag{251}$$

The difference of angles

$$\Delta = \vartheta_k - \vartheta \tag{252}$$

is given to first order by

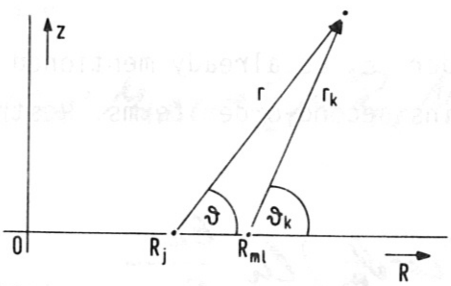

Fig. 13

$$\Delta = (R_{ml} - R_j)/r_k . \tag{253}$$

In Sections 5.3 and 5.4.1 to 5.4.4 the flux functions ψ_j are given as functions of the normalized coordinate ρ and the angular coordinate ϑ. For the present calculations it is conventient to omit ρ by using (136), thus introducing the radial coordinate r and the minor radius r_j (replace r_a by r_i in (136)). To evaluate (250) we have to proceed according to the following scheme:

$$\psi_j(r,\vartheta) = \psi_j(r = r_k + \Delta R \cos\vartheta_k, \vartheta = \vartheta_k - \Delta).$$

By Taylor expansions around r_k and ϑ_k and restriction to terms up to first order in ε we get the result

$$\begin{aligned} M_{j,ml} = \frac{N_{mz}}{I_j}\Big[&\psi_j(r_{mz},\vartheta_m) - \psi_j(r_{me},\vartheta_m) + \\ &\Delta R\Big[\frac{\partial\psi_j}{\partial r}(r_{mz},\vartheta_m) - \frac{\partial\psi_j}{\partial r}(r_{me},\vartheta_m)\Big]\cos\vartheta_m - \\ &\Delta\vartheta\Big[\frac{\partial\psi_j}{\partial\vartheta}(r_{mz},\vartheta_m) - \frac{\partial\psi_j}{\partial\vartheta}(r_{me},\vartheta_m)\Big]\Big]. \end{aligned} \tag{254}$$

5.6.1 Plasma-magnetic limiter inductance

The flux function ψ_{pl} outside the plasma is given by (164). Upon inserting $\rho = r/r_{pl}$ in ψ_{pl} we can evaluate (254). The result is

$$\begin{aligned} M_{pl,ml} = M_{14} = \mu_0 R_{pl} N_{mz}\Big[&\Big(1 + \frac{\varepsilon_{mz}}{2}\cos\vartheta_m\Big)\ln\frac{\varepsilon_{me}}{\varepsilon_{mz}} \\ &+ \frac{1}{2}(\varepsilon_{mz} - \varepsilon_{me})\Big[\varepsilon_{pl}\Big(\ln\frac{8R_{pl}}{r_{me}} - 1\Big) - \frac{\varepsilon_{pl}}{\varepsilon_{mz}\varepsilon_{me}}\Big(\lambda_1 + \frac{1}{2}\Big) \\ &+ \frac{2}{\varepsilon_{mz}\varepsilon_{me}\varepsilon_{pl}}\big(R_{ml}/R_{pl} - 1\big)\Big]\cos\vartheta_m\Big]. \end{aligned} \tag{255}$$

Because $\Delta\varepsilon = \varepsilon_{mz} - \varepsilon_{me}$ is of order ε, as already mentioned in Section 5.4.5, the formula (255) contains second-order terms. Restriction to first order leads to

$$M_{14} = M_{pl,ml} = \mu_0 R_{pl} N_{mz}\Big(1 + \frac{\varepsilon_{mz}}{2}\cos\vartheta_m\Big)\ln\frac{\varepsilon_{me}}{\varepsilon_{mz}} . \tag{256}$$

5.6.2 Transformer-magnetic limiter inductance

It is assumed that the magnetic limiter coils are placed inside the transformer coils. Because the transformer flux function $\psi_{1,tr}$ according to (174) is constant in this region the mutual inductance $M_{tr,ml}$ vanishes:

$$M_{24} = M_{tr,ml} = 0. \tag{257}$$

5.6.3 Vertical field-magnetic limiter inductance

It is again assumed that the magnetic limiter coils are situated inside the vertical field coils. The appropriate flux function $\psi_{1,v}$ is given by (184). From (254) we get

$$M_{34} = M_{v,ml} = \frac{1}{2k}\mu_0 \pi R_{ml} N_v N_{mz} \frac{\varepsilon_{mz}-\varepsilon_{me}}{\varepsilon_v} \times \left[\cos\vartheta_m + \frac{1}{\varepsilon_{mz}}\left({}^{R_v}/_{R_{ml}} - 1\right)\sin\vartheta_m + \frac{\varepsilon_{mz}-\varepsilon_{me}}{2\varepsilon_v}\cos 2\vartheta_m\right]. \tag{258}$$

Restriction to first order in ε leads to

$$M_{34} = M_{v,ml} = \frac{1}{2k}\mu_0 \pi R_{ml} N_v N_{mz} \frac{\varepsilon_{mz}-\varepsilon_{me}}{\varepsilon_v}\cos\vartheta_m . \tag{259}$$

5.6.4 Plasma chamber-magnetic limiter inductances

The magnetic limiter coils are assumed to lie inside the plasma chamber. The appropriate flux functions $\psi_{1,c0}$, $\psi_{1,c1}$, and $\psi_{1,c2}$ are given by (198) to (200). The first order results for the inductances are

$$M_{45} = M_{ml,co} = \frac{1}{2}\mu_0 R_{ml} N_{mz} (\varepsilon_{mz}-\varepsilon_{me})\left(\ln\frac{8R_c}{r_c} - \frac{1}{2}\right)\cos\vartheta_m , \tag{260}$$

$$M_{46} = M_{ml,c1} = \frac{1}{16}\mu_0 \pi R_{ml} N_{mz} \frac{\varepsilon_{mz} - \varepsilon_{me}}{\varepsilon_c} \times$$
$$[8 \cos\vartheta_m + (\varepsilon_{mz} + \varepsilon_{me})(2 + 3\cos\vartheta_m)] , \tag{261}$$

$$M_{47} = M_{ml,c2} = \frac{1}{8}\mu_0 \pi R_{ml} N_{mz} \frac{\varepsilon_{mz} - \varepsilon_{me}}{\varepsilon_c} \times$$
$$[4 \frac{\varepsilon_{mz} + \varepsilon_{me}}{\varepsilon_c} \cos 2\vartheta_m +$$
$$\frac{\varepsilon_{mz}^2 + \varepsilon_{mz}\varepsilon_{me} + \varepsilon_{me}^2 + 2\varepsilon_c^2}{\varepsilon_c} \cos\vartheta_m . \tag{262}$$

5.7 The vertical field parameters ν

In general, the current flowing in a poloidal coil a produces a vertical component B_{za} of the magnetic induction at the plasma centre $R = R_{pl}$, $z = 0$. This vertical field follows from the corresponding flux function ψ_j by using (8):

$$B_{za} = \frac{1}{2\pi R_{pl}} \cdot \frac{\partial \psi_a}{\partial R}(R = R_{pl}, z = 0) . \tag{263}$$

Because the flux functions given in Sections 5.3 and 5.4.2 to 5.4.4 are written in terms of $\rho = r/r_a$ and ϑ it is more convenient to use (134). This is possible because $B_z = B_\vartheta$ for $z = 0$. In the actual calculation the normalization $\rho = r/r_a$ and a possible shift $R_{pl}-R_a$ have to be taken into account.

For the limiter coils we directly calculate the magnetic induction produced by one coil and then sum the result over the three coils of the system. The magnetic inductions are calculated to zero order in r_{qz}/r_a, which is a good approximation because the cross-sectional dimension r_{qz} is small compared with r_{mz} and r_{me}.

The calculations for both the coils with distributed currents and the limiter coils are easily performed and yield the following results which contain terms up to first order in ε:

$$\nu_2 = \nu_{tr} = 0 \quad , \tag{264}$$

$$\nu_3 = \nu_V = \frac{\mu_0 N_V}{4\pi r_V} \quad , \tag{265}$$

$$\nu_4 = \nu_{ml} = \frac{\mu_0 N_{mz}}{2\pi r_{mz}} \left(\frac{\varepsilon_{mz}}{\varepsilon_{ml}} - 1 \right) \cos\vartheta_m \quad , \tag{266}$$

$$\nu_5 = \nu_{c0} = \frac{\mu_0}{4\pi r_c} \varepsilon_c \left(\ln 8/\varepsilon_c - 1/2 \right) , \tag{267}$$

$$\nu_6 = \nu_{c1} = \frac{\mu_0}{4 r_c} \quad , \tag{268}$$

$$\nu_7 = \nu_{c2} = \frac{\mu_0}{8 r_c} \varepsilon_c \left[1 + (4/\varepsilon_c^2) . (R_{pl}/R_c - 1) \right] . \tag{269}$$

5.8 The magnetic field at the inner edge of the transformer coil

In general, the magnetic field acting on a coil must not exceed certain limiting values in order to meet technological constraints. These may be due either to limitations of stress and strain or to the conditions a superconductor needs for safe performance. An important limitation of this kind is the so-called "core constraint" in connection with tokamak reactor designs: the flux ϕ_{tr} through the inner bore (see Fig. 14) of the transformer must not exceed an upper limit in order to prevent a s.c. transformer coil from going normal because of too high a magnetic field at the inner edge.

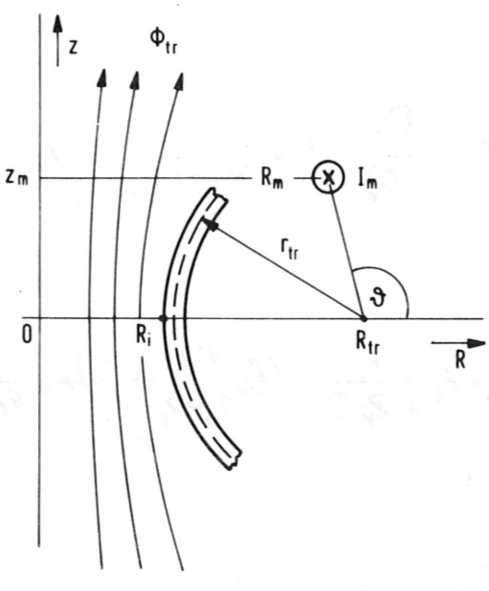

Fig. 14

All poloidal coil systems contribute to the flux ϕ_{tr} and hence to the magnetic field B_z at $R = R_i$, $z = 0$. As in the case of the vertical field produced at the plasma centre, we introduce a parameter ν which relates the magnetic induction produced to the corresponding current. The total induction at $R = R_i$, $z = 0$ is given by

$$B_z(R=R_i, z=0) = \sum_{j=1}^{7} \nu_{tj} I_j . \qquad (270)$$

The ν_{tj} for the coils with distributed current can be calculated from the corresponding flux functions, as already described in Section 5.7. Obviously this is only a reasonable approximation if R_i does not become too small relative to the components' major radii.

For the calculation of $\nu_{t,ml}$ (contribution of the magnetic limiter current I_4) we shall only use a rough approximation because the contribution is small anyway owing to the multipole character of the limiter coil triple. We determine the field produced at $R = R_i$, $z = 0$ by the current I_m from the formula

$$B_{zm} = \frac{\mu_0 I_m}{2} \cdot \frac{R_m^2}{(R_m^2 + z_m^2)^{3/2}} \qquad (271)$$

which is exact for $R_i = 0$. The relative error introduced is of the order $(R_i/R_m)^2$. By identifying I_m and R_m with the magnetic limiter ampere turns and radii and summing over the three coils we can easily calculate $\nu_{t,ml}$.

The results for the ν_{tj} up to order ε are given by

$$\nu_{t,pl} = \frac{\mu_0}{2\pi R_i} \cdot \frac{R_{pl}}{R_{pl}-R_i} \left[1 + \varepsilon_{pl} \frac{R_{pl}-R_i}{2 r_{pl}} \left(\ln \frac{8 R_{pl}}{R_{pl}-R_i} - 2 \right) - \varepsilon_{pl} \frac{r_{pl}}{2(R_{pl}-R_i)} \left(\lambda_1 + \frac{1}{2} \right) \right], \qquad (272)$$

$$\nu_{t,tr} = \frac{\mu_0}{2\pi R_i} \cdot \frac{R_{tr} N_{tr}}{R_{tr}-R_i} \left[1 + \varepsilon_{tr} \frac{R_{tr}-R_i}{2 r_{tr}} \left(\ln \frac{8 R_{tr}}{R_{tr}-R_i} - 2 \right) - \varepsilon_{tr} \frac{r_{tr}}{2(R_{tr}-R_i)} \left(\ln \frac{8 R_{tr}}{r_{tr}} - 1 \right) \right], \qquad (273)$$

$$\nu_{t,v} = \frac{\mu_0}{2\pi R_i} \cdot \frac{R_v N_v}{R_v-R_i} \left[\frac{r_v}{2(R_v-R_i)} + \frac{\alpha r_v^2}{2(R_v-R_i)^2} - \varepsilon_v \frac{r_v}{4(R_v-R_i)} \left(\ln \frac{8 R_v}{R_v-R_i} + \frac{1}{2} \right) + \varepsilon_v \frac{r_v^2}{8(R_v-R_i)^2} \right], \qquad (274)$$

$$\nu_{t,co} = \frac{\mu_0}{2\pi R_i} \cdot \frac{R_c}{R_c-R_i} \left[1 + \varepsilon_c \frac{R_c-R_i}{2 r_c} \left(\ln \frac{8 R_c}{R_c-R_i} - 2 \right) - \varepsilon_c \frac{r_c}{4(R_c-R_i)} \right], \qquad (275)$$

$$v_{t,c1} = \frac{\mu_0}{2R_i}\cdot\frac{R_c}{R_c-R_i}\left[-\frac{r_c}{2(R_c-R_i)} - \varepsilon_c\frac{r_c}{4(R_c-R_i)}\left(\ln\frac{8R_c}{R_c-R_i}+\frac{1}{2}\right) + \varepsilon_c\frac{r_c^2}{8(R_c-R_i)^2}\right], \quad (276)$$

$$v_{t,c2} = \frac{\mu_0}{R_i}\cdot\frac{R_c}{R_c-R_i}\left[\frac{r_c^2}{(R_c-R_i)^2} - \varepsilon_c\frac{3r_c}{8(R_c-R_i)}\right], \quad (277)$$

$$v_{t,ml} = -\frac{\mu_0}{2R_{ml}} N_{mz}(\varepsilon_{mz}-\varepsilon_{ml})\cos\vartheta_m . \quad (278)$$

5.9 The relation between plasma current and magnetic limiter current

In Section 3.3 we introduced a factor f of proprotionality between the plasma current and the magnetic limiter current by equation (66):

$$I_{ml} = f \cdot I_{pl} . \quad (279)$$

This factor f depends on the plasma and magnetic limiter geometries as well as on the position of the stagnation point S (see Fig. 15).

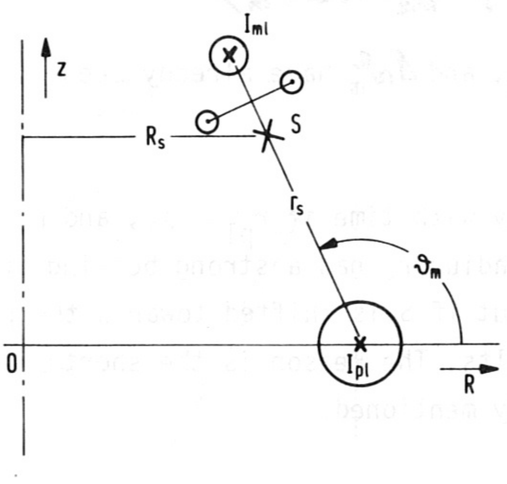

Fig. 15

The stagnation point is defined as that location where the ϑ-components of the magnetic inductions produced by the plasma and the magnetic limiter coil triple just cancel each other:

$$B_{\vartheta,pl} + B_{\vartheta,ml} = 0 . \quad (280)$$

Because of the short range of the multipole field we can neglect the contribution of a second multipole triple, which may be situated symmetrically with respect to the plane $z = 0$ if ϑ_m is not close to zero.

$B_{\vartheta,pl}$ follows from

$$B_{\vartheta,pl} = \frac{1}{2\pi R_s} \cdot \frac{\partial \psi_{pl}}{\partial r} \tag{281}$$

with ψ_{pl} given by (164). We assume here that the plasma is centred at $R = R_{pl} = R_{ml}$ and $z = 0$.

The field $B_{\vartheta,ml}$ is calculated by treating the multipole rings as straight conductors. This is possible owing to the large aspect ratio of the rings and because we only need the field in the vicinity of the conductors.

The determination of both fields is straightforward and yields the B_ϑ as products of the respective currents with functions which mainly depend on geometry. By using (280) and (279) we get

$$f = \frac{1}{N_{mz}} \cdot \frac{1}{r_s\left(1 + r_s/R_{ml} \cdot \cos\vartheta_m\right)} \left[1 - \frac{1}{2}\left(\frac{r_{pl}}{R_{ml}}\right) \times \left[\frac{r_s}{r_{pl}}\left(\ln\frac{8R_{ml}}{r_s} - 2\right) - \left(\frac{r_{pl}}{r_s}\right)\left(\lambda_1 + \frac{1}{2}\right)\right]\cos\vartheta_m\right] \times \frac{(r_{mz} - r_s)(r_{me}^2 + r_s^2 - 2 r_{me} r_s \cos\Delta\vartheta_m)}{r_{me}(r_{me} - r_s\cos\Delta\vartheta_m) + r_{mz}(r_s - r_{me}\cos\Delta\vartheta_m)} \tag{282}$$

The geometrical parameters r_{mz}, r_{me}, and $\Delta\vartheta_m$ have already been introduced in Fig. 10.

Equation (282) shows that f may vary with time if r_{pl}, λ_1, and r_s do so. The minor stagnation point radius r_s has a strong bearing on f: if r_s is not close to r_{mz} and r_{me} but if S is shifted towards the plasma centre, a strong increase of f results. The reason is the short range of the multipole field already mentioned.

5.10 A heuristic correction to the zero-order inductances

A toroidal surface current component i_0 which is independent of ϑ produces a contribution to the inductances which up to first order in ε_a is given by

$$L^{(1)} = \mu_0 R_a \left(\ln 8R_a/r_a - 2\right). \tag{283}$$

We found this result in the calculation of plasma, transformer, and chamber inductances.

To infer a second-order correction to this relation, one can use the exact result for L given in /7/.

The relative difference

$$\Delta L/L^{(1)} = (L^{(1)} - L)/L^{(1)} \tag{284}$$

can easily be calculated by means of the tabulated values of L given in /7/. The result is shown in Fig. 16 as a function of $\varepsilon_a = r_a/R_a$ in a double logarithmic representation. Indeed, the correction $\Delta L/L^{(1)}$ in this logarithmic plot is very close to the straight line corresponding to

$$\Delta L/L^{(1)} = \varepsilon_a^2 . \tag{285}$$

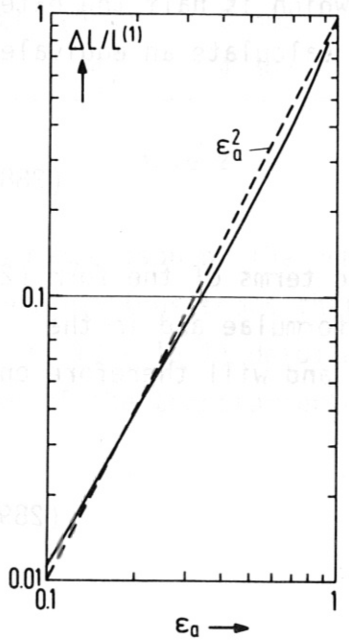

Fig. 16

By using (285), (284), and (283) we get

$$L = (1 - \varepsilon_a^2)\mu_0 R_a \left(\ln \frac{8R_a}{r_a} - 2\right). \tag{287}$$

In the logarithmic term we have not replaced R_a/r_a by $1/\varepsilon_a$ because ε_a is a measure of toroidicity, whereas the occurrence of $\ln(R_a/r_a)$ is not due to toroidicity but to the 1/r-variation of the magnetic field strength in the proximity of any line current. The factor 8 is characteristic of the geometry and may be changed if one treats the case of minor cross-sections other than circular.

To correct our results, we only have to substitute in the formulae for L_1, L_2, L_5, M_{12}, M_{15}, and M_{25} according to

$$\left(\ln\frac{8R_a}{r_a}-2\right) \rightarrow (1-\varepsilon_a^2)\left(\ln\frac{8R_a}{r_a}-2\right). \qquad (288)$$

6. A sample calculation using ASDEX parameters

6.1 Inductances

The self and mutual inductances of the ASDEX coils have been calculated numerically /8/ and can therefore be used for comparison with our analytical results. The geometrical arrangement of each individual turn of a coil and the cross-sectional dimension were taken into account. The numbers of turns in our nomenclature are:

$$N_2 = 100, \quad N_3 = 8, \quad N_4 = 8.$$

The ASDEX coils have minor cross-sections which are elongated in the z-direction. We characterize them by r_a (a = pl, tr, v, ml, c0, c1, c2), which is half the radial extension, and z_a which is half the extension in the z-direction. From these dimensions we calculate an equivalent radius

$$r_{eq,a} = (r_a \Delta z_a)^{1/2} \qquad (288)$$

which we use instead of r_a in all logarithmic terms of the form (283). The parameter ε_a used in the inductance formulae and in the correction (285) is a measure of toroidicity and will therefore only be based on r_a:

$$\varepsilon_a = r_a / R_a \qquad (289)$$

as was done throughout this report. If minor radii occur in the first-order contributions to the inductances, we identify them with the corresponding radial extensions r_a and hence neglect the effect of axial elongation.

In Table 2 we present the numerically calculated ASDEX inductances and the corresponding values calculated with the formulae presented in this report. Because it is convenient in practical applications to use ampereturns and voltages per turn instead of currents and voltages, we use the adequate form of inductances:

$$l_a = 1/N_a^2 . L_a \quad , \tag{290}$$

$$m_{ab} = 1/N_a N_b . M_{ab} \tag{291}$$

inductance		numerical value [μH]	analytic value [μH]
pl	(1)	3.703	3.439
pl-tr	(1-2)	0.843	0.928
pl-v	(1-3)	0.895	0.904
pl-ml	(1-4)	0.356	0.403
tr	(2)	0.841	0.928
tr-v	(2-3)	0.001	0
tr-ml	(2-4)	0.001	0
v	(3)	5.083	4.360
v-ml	(3-4)	0.002	0.009
ml	(4)	4.363	4.328

Table 2

Because the ampereturns of the various coils are of similar magnitude, it is possible to access the relative inportance of the inductances on the basis of the l_a and m_{ab}. Table 2 shows that all mutual inductances which involve at least one dipole or multipole coil are of minor importance.

The comparison of the numerical ASDEX results with our analytical approximations shows that the deviations remain of moderate size (up to 10 - 15 %) despite the large ε-values (up to 0.45 in the case of the transformer).

In all cases where l_i and β_{pol} had to be specified we used $l_i = 0.5$ (square current profile) and $\beta_{pol} = 1$. The inductances involving the chamber components are not given because no numerical values are available for comparison. This is due to the fact that the complicated ASDEX vessel was treated numerically by subdividing it into a large number (about 100) of inductively coupled circular coils /9/.

6.2 A circuit calculation

For a typical circuit calculation we adopted the following input functions:

$$I_{pl}(t) = I_1(t) = I_{plo} \cdot (1-e^{-t/\tau}), \quad (292)$$

$$r_{pl}(t) = r_{plo} \cdot (0.1 + 0.9\, t/\tau_b), \quad (293)$$

$$R_{pl}(t) = R_{plo} = \text{const}, \quad (294)$$

$$\beta_{pol}(t) = \beta_{po} = \text{const}, \quad (295)$$

$$R_1(t) = R_{1o} \cdot [(f_o-1)\, e^{-t/\tau} + 1], \quad (296)$$

with

$\tau = 10^{-2}$ s, $\quad r_{plo} = 0.4$ m, $\quad R_{1o} = 10^{-6}\,\Omega$,

$\tau_b = 10^{-1}$ s, $\quad R_{plo} = 1.65$ m, $\quad f_o = 10^3$

$I_{plo} = 5 \cdot 10^5$ A $\quad \beta_{po} = 1$,

Further data are:

$\sigma_c = 0.95 \cdot 10^6$ $1/\Omega$m

d_c = 1 mm (chamber wall thickness)

n_v = 1 (vertical field index),

$\vartheta_m = 100^0$ (see Fig. 10),

$\Delta\vartheta_m = 20^0$ (see Fig. 10),

r_s = 0.47 m (minor stagnation point radius; see Fig. 15),

$I_{tr}(0) = I_2(0) = 0,$ $R_2 = 1.27 \times 10^{-2}\,\Omega$,

$I_{co}(0) = I_5(0) = 0,$ $R_3 = 2.25 \times 10^{-3}\,\Omega$,

$I_{c1}(0) = I_6(0) = 0,$ $R_4 = 1.33 \times 10^{-3}\,\Omega$.

$I_{c2}(0) = I_7(0) = 0.$

The vessel was assumed to have a poloidal slit leading to $I_{c5} = I_5 \equiv 0$.

Figure 17 shows some results of the computer program PCOILS, which was set up on the basis of the material presented in this report:

The magnetic limiter current $I_{ml}(t)$ essentially follows the prescribed plasma current $I_{pl}(t)$. Strict proportionality of the two currents is prevented because r_{pl}, and hence f, depends on t.

The necessary transformer current I_{tr} passes a minimum and then rises again, which leads to a reversal of the power delivered by the transformer power supply, which has to supply the voltage U_{tr}. The power reversal is due to the decrease of the plasma inductance L_1, which is produced by the linear increase of r_{pl} with t.

The vertical field current I_v, which is necessary to keep the plasma centre at its equilibrium position R_{pl} = 1.65 m, z = 0, behaves similarly to I_{tr}. The reason is again the variation of r_{pl} with t, which now mainly acts via the vertical field parameter ν given by (60).

The chamber current I_{c1} reaches a maximum value of about 20 kA, whereas I_{c2} is virtually zero. This means that the chamber current density i_c given by (196) varies as $\cos\vartheta$ along the minor circumference ($I_{co} \equiv 0$ because of the slit assumed). The L/R time of the vessel is of the order of a few 10^{-4} s, which means that the time variation of I_{c1} is essentially determined by $\dot{I}_{pl}$, $\dot{I}_{tr}$, and $\dot{I}_v$.

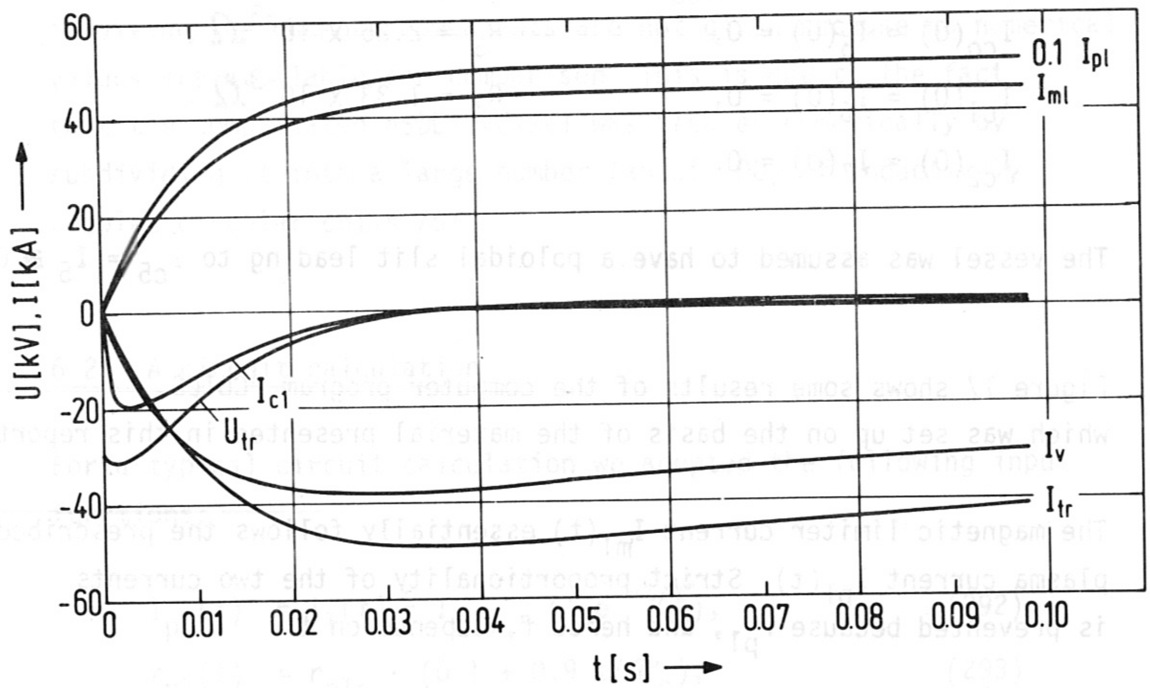

Fig. 17

7. Concluding remarks

The analytical formulae for the circuit parameters and the circuit equations presented in this report we used to set up the computer model PCOILS (pulsed coils), which describes the pulsed coil systems of tokamak reactors. After coupling with numerical plasma models such as NUDIPLAS /2/ or WHIST, the model PCOILS forms part of the tokamak power plant model SISYFUS elaborated by the IPP project systems studies. The computer program PCOILS will be described in a separate report.

Acknowledgements

The author gratefully acknowledges discussions contributed by K. Borrass, H. Preis, and P. Martin. All programming work and the numerical calculations were performed by H. Gorenflo.

References

/1/ K. Borraß, R. Bünde, W. Dänner: "First results with the SISYFUS code: The influence of plasma impurities on the performance of Tokamak power plants", Proc. the Technology of Controlled Nuclear Fusion Conference, Santa Fê, 1978

/2/ K. Borraß: "A zero dimensional tokamak transport model. Part I - General description". IPP-Report IPP 4/146, August 1977

/3/ V.S. Mukhovatov, V.D. Shafranov: "Plasma equilibrium in a tokamak", Nucl. Fus., 11 (1971), 605

/4/ Y. Suzuki et al.: "Tokamak circuit theory", JAERI-Report JAERI-M 6531, 1976 (Culham translation CTO/1449)

/5/ H. Hak: "Eisenlose Drosselspulen", Koehler Verlag, Leipzig, 1938

/6/ K. Simonyi: "Theoretische Elektrotechnik", Deutscher Verlag der Wissenschaften, Berlin 1977

/7/ J.H. Malmberg, M.N. Rosenbluth: "High frequency inductance of a torus", Rev. Scient. Instrum., 36, 12 (1965), 1886

/8/ H. Preis, P. Martin: Private communication of the inductance values calculated numerically for the IPP tokamak ASDEX by means of the computer program HEDO

/9/ H. Preis: "Calculation of voltages and currents induced in the vacuum vessel of ASDEX by plasma disruptions", 10th Symposium on Fusion Technology, Padua, Sept. 1978